Inorg. Chem. **2007**, *46*, 8897–8912

Copper(I) Cyanide Networks: Synthesis, Luminescence Behavior and Thermal Analysis. Part 1. Diimine Ligands

Tristan A. Tronic, Kathryn E. deKrafft, Mi Jung Lim, Amanda N. Ley, and Robert D. Pike*

Department of Chemistry, College of William and Mary, Williamsburg, Virginia 23187-8795

Received April 13, 2007

Metal–organic networks of CuCN with diimines (L) = pyrazine (Pyz), 2-aminopyrazine ($PyzNH_2$), quinoxaline (Qox), phenazine (Phz), 4,4′-bipyridyl (Bpy), pyrimidine (Pym), 2-aminopyrimidine ($PymNH_2$), 2,4-diaminopyrimidine ($Pym(NH_2)_2$), 2,4,6-triaminopyrimidine ($Pym(NH_2)_3$), quinazoline (Qnz), pyridazine (Pdz), and phthalazine (Ptz) were studied. Open reflux reactions produced complexes $(CuCN)_2(L)$ for L = Qox, Phz, Bpy, $PymNH_2$, $Pym(NH_2)_2$, Qnz, and Pdz and $(CuCN)_3(L)$ complexes for L = Pyz, $PyzNH_2$, Qox, Bpy, $Pym(NH_2)_3$, and Pdz. Also produced were $(CuCN)_3(Pyz)_2$, $(CuCN)(PyzNH_2)$, $(CuCN)_7(Pym)_2$, $(CuCN)_5(Qnz)_2$ and $(CuCN)_5(Ptz)_2$. X-ray structures are presented for $(CuCN)_2(Pdz)$, $(CuCN)_2(PymNH_2)$, and $(CuCN)_7(Pym)_2$. Hydrothermal reactions yielded additional X-ray structures of $(CuCN)_2(PyzNH_2)$, $(CuCN)_3(Pym(NH_2)_2)$, $(CuCN)_4(Qnz)$, a second $(CuCN)_2(Pdz)$ phase, $(CuCN)_5(Pdz)_2$, $(CuCN)_2(Ptz)$, and $(CuCN)_7(Ptz)_2$. Structural trends, including cuprophilic interactions and cyano-bridged $Cu_2(CN)_2$ dimer formation, are discussed. Particularly short Cu···Cu interactions are noted for the novel 4- and 5-coordinate $Cu_2(CN)_2$ dimers. Thermal analyses show that most of the complexes decompose with loss of L around 160–180 °C. Luminescence behavior is relatively weak in the products.

Introduction

Metal−organic networks are of great interest due to potential applications in separations, gas storage, and catalysis.[1] Metal−organic materials based on luminescent metals, such as copper(I) or lanthanides, have potential in gas molecule sensing systems, since absorption of small molecules into the network can potentially alter its luminescence behavior.[2] Formation of networks having significant porosity is crucial to such technologies. However, entrainment of anions and/or solvent molecules, or even the interpenetration of the network itself, often serves to fill the pores in metal−organic networks. Networks produced from metal salts of bridging anions, such as halides and pseudohalides, can be effectively used to avoid the problem of counterions filling pores. We have recently been studying network materials derived from copper(I) halides.[3] However, the resistance of copper(I) halides toward oxidation is modest at best. In contrast, CuCN is highly resistant to oxidation. In addition, cyanide bridging of metal centers is well established, producing robust and uniformly porous materials.[4] Therefore, we undertook a study of the networks formed by CuCN with the diimine ligands (L) shown in Chart 1. Additional study of CuCN with diamine ligands will be communicated separately.[5]

* To whom correspondence may be sent. Telephone: 757-2212555. Fax: 757-2212715. E-mail address: rdpike@wm.edu.

(1) Muller, U.; Schubert, M.; Teich, F.; Puetter, H.; Schierle-Arndt, K.; Pastré, J. *J. Mater. Chem.* **2006**, *16*, 626. (b) Dincă, M.; Yu, A. F.; Long, J. R. *J. Am. Chem. Soc.* **2006**, *128*, 8904. (c) Rowsell, J. L. C.; Yaghi, O. M. *J. Am. Chem. Soc.* **2006**, *128*, 1304. (d) Forster, P. M.; Cheetham, A. K. *Top. Catal.* **2003**, *24*, 79. (e) Kesanli, B.; Lin, W. *Coord. Chem. Rev.* **2003**, *246*, 305.

(2) (a) Exstrom, C. L.; Sowa, J. L., Jr.; Daws, C. A.; Janzen, D.; Mann, K. R.; Moore, G. A.; Stewart, F. F. *Chem. Mater.* **1995**, *7*, 15. (b) Daws, C. A.; Exstrom, C. L.; Sowa, J. L., Jr.; Mann, K. R. *Chem. Mater.* **1997**, *9*, 363. (c) Vickery, J. C.; Olmstead, M. M.; Fung, E. Y.; Balch, A. L. *Angew. Chem., Int. Ed.* **1997**, *36*, 1179. (d) Cariati, E.; Bu, X.; Ford, P. C. *Chem. Mater.* **2000**, *12*, 3385. (e) Drew, S. M.; Janzen, D. E.; Buss, C. E.; MacEwen, D. I.; Dublin, K. I.; Mann, K. R. *J. Am. Chem. Soc.* **2001**, *123*, 8414. (f) Buss, C. E.; Mann, K. R. *J. Am. Chem. Soc.* **2002**, *124*, 1031. (g) Fernández, E. J.; López-de-Luzuriaga, J. M.; Monge, M.; Olmos, M. E.; Pérez, J.; Laguna, A.; Mohamed, A. A.; Fackler, J. P., Jr. *J. Am. Chem. Soc.* **2003**, *125*, 2022. (h) Lu, W.; Chan, M. C. W.; Zhu, N.; Che, C.-M.; He, Z.; Wong, K.-Y. *Chem.-Eur. J.* **2003**, *9*, 6155.

(3) (a) Graham, P. M.; Pike, R. D.; Sabat, M.; Bailey, R. D.; Pennington, W. T. *Inorg. Chem.* **2000**, *39*, 5121. (b) Pike, R. D.; Borne, B. D.; Maeyer, J. T.; Rheingold, A. L. *Inorg. Chem.* **2002**, *41*, 631. (c) Maeyer, J. T.; Johnson, T. J.; Smith, A. K.; Borne, B. D.; Pike, R. D.; Pennington, W. T.; Krawiec, M.; Rheingold, A. L. *Polyhedron* **2003**, *22*, 419. (d) Pike, R. D.; Reinecke, B. A.; Dellinger, M. E.; Wiles, A. B.; Harper, J. D.; Cole, J. R.; Dendramis, K. A.; Borne, B. D.; Harris, J. L.; Pennington, W. T. *Organometallics* **2004**, *23*, 1986. (e) Wiles, A. B.; Pike, R. D. *Organometallics* **2006**, *25*, 3282.

(4) (a) Kaye, S. S.; Long, J. R. *Catal. Today* **2007**, *120*, 311. (b) Culp, J. T.; Park, J.-H.; Frye, F.; Huh, Y.-D.; Meisel, M. W.; Talham, D. R. *Coord. Chem. Rev.* **2005**, *249*, 2642. (c) Dunbar, K. R.; Heintz, R. A. *Prog. Inorg. Chem.* **1997**, *45*, 283.

10.1021/ic7007057 CCC: $37.00
Published on Web 09/13/2007

Chart 1

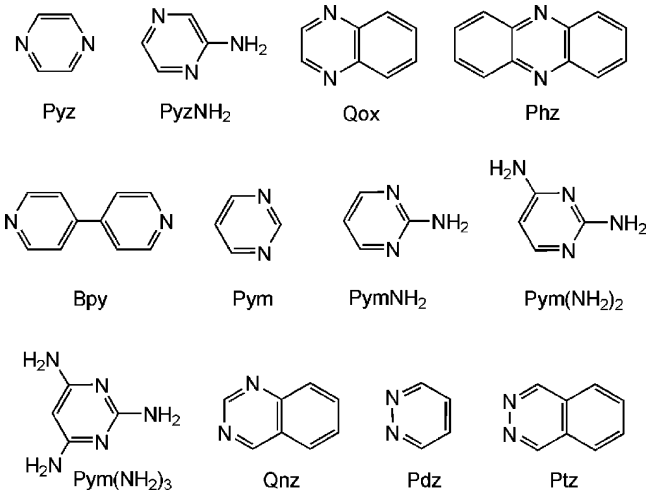

A number of two-dimensional (2D) and three-dimensional (3D) diamine and diimine-bridged networks of CuCN are already known.[6−22] However, as suggested by the structural characterization of 10 new networks (including isomeric phases) in this contribution, it is apparent that there exists in the CuCN−L system a great wealth of materials. The known complexes exhibit a variety of CuCN:L ratios including 1:1, 3:2, 2:1, 3:1, 7:2, and 4:1. In a few cases (e.g., L = Bpy), two or more stoichiometric ratios have been encountered.[12−15,18] Not surprisingly, all of the known CuCN−L complexes are 2D and 3D networks. In addition, numerous 1D CuCN polymers supported by monodentate or chelating nitrogen ligands are recognized.[23,24] The prevailing methods of synthesis for these materials are (1) hydrothermal (HT) reactions (125−200 °C),[10−12,18] (2) reactions in acetonitrile (20−100 °C),[13−17] (3) neat reactions,[6,14] and (4) aqueous ligand exchange.[7−9] Surprisingly little attention has been devoted to atmospheric pressure aqueous reactions of CuCN with bridging ligands, L. It is to be expected that the substantial drawbacks of HT synthesis (including small reaction scales, modest yields, and mixed products) can be avoided through the application of open reflux conditions. The study detailed below involves of the production of CuCN−L networks via open reflux reactions in water. In addition, we employed HT conditions in parallel syntheses. This was done for two reasons: (1) to produce single crystals (where possible) and (2) to make comparisons with known CuCN work, much of which has been carried out under HT conditions.

Experimental Section

Materials and Methods. All reagents were purchased from Aldrich or Acros and used without purification, except for Qox, which was sublimed before use. All water used was ultrafiltered, deionized quality and was thoroughly degassed with Ar. Analyses for C, H, and N were carried out by Atlantic Microlabs, Norcross, GA, and Cu analyses were carried out using a Perkin-Elmer AAnalyst 700 atomic absorption instrument as previously described.[3a] Luminescence measurements were carried out in reflectance mode on well-ground powders using a Perkin-Elmer LS 55 spectrofluorimeter. IR measurements were made on KBr pellets using a Digilab FTS 7000 FTIR spectrophotometer. Thermogravimetric analyses (TGA) were conducted using a TA Instruments Q500 in the dynamic (variable temperature) mode with a maximum heating rate of 50 °C/min to 900 °C under 60 mL/min N_2 flow.

Reflux Syntheses. $(CuCN)_3(Pyz)_2$, 1a. Copper(I) cyanide (1.79 g, 20.0 mmol) and KCN (1.30 g, 20.0 mmol) were suspended in 50 mL of H_2O and warmed. Pyz was added (0.801 g, 10.0 mmol), and the resulting suspension was refluxed under N_2 overnight. The suspended solid was collected by means of filtration, washed with H_2O, ethanol, and diethyl ether, and then dried under vacuum. An orange powder was isolated (1.27 g, 2.97 mmol, 59.3%). IR (KBr pellet, cm^{-1}) 3078 (w), 2124 (m), 2104 (m), 1412 (s), 1161 (m), 1121 (m), 1043 (m), 793 (s). Anal. Calcd for $C_{11}H_8N_7Cu_3$: Cu, 44.5; C, 30.81; H, 1.88; N, 22.56. Found: Cu, 43.3; C, 30.80; H, 1.81; N, 22.56. TGA Calcd for $(CuCN)_3(Pyz)$: 81.4. Found: 80.7 (125−185 °C). Calcd for CuCN 62.8. Found: 62.8 (185−220 °C).

$(CuCN)_3(Pyz)$, 1b. Copper(I) cyanide (1.79 g, 20.0 mmol) and KCN (0.651 g, 10.0 mmol) were suspended in 50 mL of H_2O and warmed. Pyz was added (0.400 g, 5.0 mmol), and the resulting suspension was refluxed under N_2 overnight. The suspended solid was collected by means of filtration, washed with H_2O, ethanol, and diethyl ether, and then dried under vacuum. A yellow powder was isolated (1.53 g, 4.38 mmol, 87.6%). IR (KBr pellet, cm^{-1}) 2152 (m), 2121 (m), 1416 (m), 1161 (w), 1124 (w), 1045 (m), 800 (w). Anal. Calcd for $C_7H_4N_5Cu_3$: Cu, 54.7; C, 24.11; H, 1.16; N,

(5) Pike, R. D.; deKrafft, K. E.; Ley, A. N.; Tronic, T. A. *Chem. Commun.* **2007**, 3732−3734.
(6) Cromer, D. T.; Larson, A. C. *Acta. Crystallogr., Sect. B* **1972**, *28*, 1052.
(7) Stocker, F. B. *Inorg. Chem.* **1991**, *30*, 1472.
(8) (a) Stocker, F. B.; Troester, M. A.; Britton, D. *Inorg. Chem.* **1996**, *35*, 3145. (b) Stocker, F. B.; Troester, M. A. *Inorg. Chem.* **1996**, *35*, 3154.
(9) Stocker, F. B.; Staeva, T. P.; Rienstra, C. M.; Britton, D. *Inorg. Chem.* **1999**, *38*, 984.
(10) Chesnut, D. J.; Kusnetzow, A.; Zubieta, J. *J. Chem. Soc., Dalton Trans.* **1998**, 4081.
(11) (a) Chesnut, D. J.; Kusnetzow, A.; Birge, R. R.; Zubieta, J. *Inorg. Chem.* **1999**, *38*, 2663. (b) Chesnut, D. J.; Kusnetzow, A.; Birge, R. R.; Zubieta, J. *Inorg. Chem.* **1999**, *38*, 5484.
(12) Chesnut, D. J.; Plewak, D.; Zubieta, J. *J. Chem. Soc., Dalton Trans.* **2001**, 2567.
(13) Teichert, O.; Sheldrick, W. S. *Z. Anorg. Allg. Chem.* **2000**, *626*, 1509.
(14) Teichert, O.; Sheldrick, W. S. *Z. Anorg. Allg. Chem.* **1999**, *625*, 1860.
(15) Greve, J.; Näther, C. *Z. Naturforsch.* **2004**, *59b*, 1325.
(16) Mühle, J.; Sheldrick, W. S. *Z. Anorg. Allg. Chem.* **2003**, *629*, 2097.
(17) Kromp, T.; Sheldrick, W. S.; Näther, C. *Z. Anorg. Allg. Chem.* **2003**, *629*, 45.
(18) Hibble, S. J.; Chippindale, A. M. *Z. Anorg. Allg. Chem.* **2005**, *631*, 542.
(19) Kuhlman, R.; Schimek, G. L.; Kolis, J. W. *Polyhedron* **1999**, *18*, 1379.
(20) Colacio, E.; Domínguez-Vera, J. M.; Lloret, F.; Moreno Sánchez, J. M.; Kivekäs, R.; Rodríguez, A.; Silanpää, R. *Inorg. Chem.* **2003**, *42*, 4209.
(21) Jess, I.; Näther, C. *Acta. Crystallogr., Sect. E* **2006**, *62*, m721.
(22) Hanika-Heidl, H.; Etaiw, S. E. H.; Ibrahim, M. S.; El-din, A. S. B.; Fischer, R. D. *J. Organomet. Chem.* **2003**, *684*, 329.
(23) Examples include: (a) Morpurgo, G. O.; Dessy, G.; Fares, V. *J. Chem. Soc., Dalton Trans.* **1984**, 785. (b) Dyason, J. C.; Healy, P. C.; Englehardt, L. M.; Pakawatchai, C.; Patrick, V. A.; White, A. H. *J. Chem. Soc., Dalton Trans.* **1985**, 839. (c) Olmstead, M. M.; Speier, G.; Szabo, L. *Acta. Crystallogr., Sect. C* **1993**, *49*, 320. (d) Stocker, F. B.; Troester, M. A.; Britton, D. *J. Chem. Crystallogr.* **2000**, *30*, 389. (e) Chesnut, D. J.; Kusnetzow, A.; Birge, R. R.; Zubieta, J. *J. Chem. Soc., Dalton Trans.* **2001**, 2581. (f) Yu, J.-H.; Xu, J.-Q.; Yang, Q.-Pan, X., L.-Y.; Wang, T.-G.; Lu, C.-H.; Ma, T.-H. *J. Mol. Struct.* **2003**, *658*, 1. (g) Yu, J.-H.; Ren, Z.-G.; Li, H.-X.; Zhang, W.-H.; Chen, J.-X.; Zhang, Y.; Lang, J.-P. *J. Mol. Struct.* **2006**, *782*, 150. (h) Song, Y.; Xu, Y.; Wang, T.- W.; Wang, X.-W.; You, X.-Z. *J. Mol. Struct.* **2006**, *788*, 206.
(24) Bowmaker, G. A.; Lim, K. C.; Skelton, B. W.; White, A. H. *Z. Naturforsch.* **2004**, *59b*, 1264.

20.08. Found: Cu, 54.2; C, 24.35; H, 1.14; N, 20.08. TGA Calcd for CuCN: 77.0. Found: 77.5 (195−235 °C).

(CuCN)(PyzNH$_2$), 2a. The procedure was identical to that used for **1a** using PyzNH$_2$ instead of Pyz. A yellow powder was isolated (84.0%). IR (KBr pellet, cm^{-1}) 3436 (m), 3337 (m), 2091 (m), 1622 (m), 1528 (m), 1435 (m), 1217 (w), 820 (w). Anal. Calcd for $C_5H_5N_4Cu$: Cu, 34.4; C, 32.52; H, 2.73; N, 30.34. Found: Cu, 33.8; C, 32.89; H, 2.69; N, 30.27. TGA Calcd for $(CuCN)_2$-(PyzNH$_2$): 74.3. Found: 74.3 (155−190 °C). Calcd for CuCN: 48.6 Found 48.8 (195−225 °C).

(CuCN)$_3$(PyzNH$_2$), 2b. The procedure was identical to that used for **1b** using PyzNH$_2$ instead of Pyz. A yellow powder was isolated (86.6%). IR (KBr pellet, cm^{-1}) 3428 (s), 3329 (s), 2079 (s), 1622 (s), 1528 (s), 1435 (s), 1213 (m), 1067 (w), 1024 (w), 823 (w). Anal. Calcd for $C_7H_5N_6Cu_3$: C, 23.11; H, 1.39; N, 23.10. Found: C, 23.37; H, 1.50; N, 23.17. TGA Calcd for CuCN: 73.9. Found: 72.7 (195−235 °C).

(CuCN)$_2$(Qox), 3a. The procedure was identical to that used for **1a** using Qox instead of Pyz. An orange powder was isolated (46.1%). IR (KBr pellet, cm^{-1}) 3071 (w), 2122 (s), 1501 (m), 1359 (w), 1209 (w), 1130 (w), 1047 (m), 946 (w), 862 (w), 759 (m). Anal. Calcd for $C_{10}H_6N_4Cu_2$: Cu, 41.1; C, 38.84; H, 1.96; N, 18.12. Found: Cu, 40.4; C, 38.67; H, 1.87; N, 17.85. TGA Calcd for CuCN: 57.9. Found: 58.2 (165−225 °C).

(CuCN)$_3$(Qox), 3b. The procedure was identical to that used for **1b** using Qox instead of Pyz. An orange powder was isolated (90.0%). IR (KBr pellet, cm^{-1}) 2125 (s), 1501 (m), 1207 (m), 1130 (w), 1047 (m), 964 (w), 860 (w), 760 (m). Anal. Calcd for $C_{11}H_6N_5$-Cu_3: Cu, 47.8; C, 33.13; H, 1.52; N, 17.56. Found: Cu, 47.8; C, 34.54; H, 1.68; N, 17.78. TGA Calcd for CuCN: 67.4. Found: 65.9 (175−225 °C).

(CuCN)$_2$(Phz), 4a. The procedure was identical to that used for **1a** using Phz instead of Pyz and using a 1:1 mixture of H_2O:EtOH as solvent. A black powder was isolated (37.6%). IR (KBr pellet, cm^{-1}) 2139 (m), 1514 (m), 1432 (w), 1370 (w), 1119 (w), 829 (w), 749 (s). Anal. Calcd for $C_{14}H_8N_4Cu_2$: Cu, 35.4; C, 46.80; H, 2.24; N, 15.59. Found: Cu, 35.0; C, 46.68; H, 2.23; N, 15.38. TGA Calcd for CuCN: 49.9. Found: 50.0 (195−245 °C).

(CuCN)$_2$(Bpy), 5a. The procedure was identical to that used for **1a** using Bpy instead of Pyz. A yellow powder was isolated (48.5%). IR (KBr pellet, cm^{-1}) 3046 (w), 2120 (s), 2096 (s), 1598 (s), 1530 (w), 1483 (w), 1408 (m), 1217 (m), 1072 (w), 1005 (w), 810 (s). Anal. Calcd for $C_{12}H_8N_4Cu_2$: Cu, 37.9; C, 42.98; H, 2.40; N, 16.71. Found: Cu, 38.3; C, 42.73; H, 2.41; N, 16.46. TGA Calcd for $(CuCN)_7(Bpy)_2$: 80.0. Found: 79.9 (225−260 °C). Calcd for CuCN: 53.4. Found: 53.4 (260−325 °C).

(CuCN)$_3$(Bpy), 5b. The procedure was identical to that used for **1b** using Bpy instead of Pyz. A yellow powder was isolated (90.3%). IR (KBr pellet, cm^{-1}) 2120 (m), 2093 (m), 1599 (m), 1530 (w), 1408 (w), 1215 (w), 1065 (w), 808 (m), 629 (w). Anal. Calcd for $C_{13}H_8N_5Cu_3$: Cu, 44.9; C, 36.75; H, 1.90, N 16.48. Found: Cu, 43.8; C, 37.35; H, 2.03; N, 16.48. TGA Calcd for $(CuCN)_9(Bpy)_2$: 87.7. Found: 89.1 (215−260 °C). Calcd for CuCN: 63.2. Found: 62.5 (260−325 °C).

(CuCN)$_7$(Pym)$_2$, 6a. The procedure was identical to that used for **1b** using Pym instead of Pyz. A yellow crystalline solid was isolated (70.0%). IR (KBr pellet, cm^{-1}) 2136 (w) 2113 (w), 2091 (w), 1559 (m), 1400 (m), 825 (w), 704 (m), 650 (w). Anal. Calcd for $C_{15}H_8N_{11}Cu_7$: Cu, 56.6; C, 22.89; H, 1.02, N 19.57. Found: Cu, 56.5; C, 22.87; H, 0.98; N, 19.56. TGA Calcd for CuCN: 79.6. Found: 79.6 (200−225 °C).

(CuCN)$_2$(PymNH$_2$), 7a. The procedure was identical to that used for **1a** using PymNH$_2$ instead of Pyz. A cream powder was isolated (41.6%). IR (KBr pellet, cm^{-1}) 3427 (m), 3327 (m), 2128 (m) 1617 (s), 1574 (m) 1462 (m), 1351 (w), 1195 (w), 808 (w), 792 (w), 665 (w). Anal. Calcd for $C_6H_5N_5Cu_2$: Cu, 46.3; C, 26.28; H, 1.84; N, 25.54. Found: Cu, 46.0; C, 26.56; H, 1.81; N, 25.39. TGA Calcd for CuCN: 65.3. Found: 65.5 (180−230 °C).

(CuCN)$_2$(Pym(NH$_2$)$_2$), 8a. The procedure was identical to that used for **1a** using Pym(NH$_2$)$_2$ instead of Pyz. A cream powder was isolated (43.0%). IR (KBr pellet, cm^{-1}) 3460 (s), 3422 (m), 3348 (w), 3325 (s), 2112 (s), 1653 (m), 1607 (s), 1556 (w), 1490 (m), 1461 (m), 1391 (w), 1267 (w), 801 (w). Anal. Calcd for $C_6H_6N_6$-Cu_2: Cu, 43.9; C, 24.92; H, 2.09; N, 29.05. Found: Cu, 43.8; C, 25.04; H, 1.96; N, 29.15.

(CuCN)$_3$(Pym(NH$_2$)$_3$), 9a. The procedure was identical to that used for **1a** using Pym(NH$_2$)$_3$ instead of Pyz. A cream powder was isolated (37.7%). IR (KBr pellet, cm^{-1}) 3467 (m), 3418 (m), 3349 (m), 3326 (m), 2141 (m), 2118 (m), 1622 (s), 1588 (s), 1555 (m), 1476 (w), 1441 (m), 1251 (w), 787 (w). Anal. Calcd for $C_7H_7N_8$-Cu_3: Cu, 48.4; C, 21.35; H, 1.79; N, 28.45. Found: Cu, 48.3; C, 21.49; H, 1.71; N, 28.57.

(CuCN)$_2$(Qnz), 10a. The procedure was identical to that used for **1a** using Qnz instead of Pyz. An orange powder was isolated (44.8%). IR (KBr pellet, cm^{-1}) 3447 (s), 3358 (s), 3315 (s) 2122 (s), 1618 (m), 1578 (m), 1491 (w), 1379 (w), 787 (m), 754 (m). Anal. Calcd for $C_{10}H_6N_4Cu_2$: Cu, 41.1; C, 38.84; H, 1.96; N, 18.12. Found: Cu, 41.1; C, 39.11; H, 1.92; N, 18.21. TGA Calcd for CuCN: 57.9. Found: 58.2 (165−220 °C).

(CuCN)$_5$(Qnz)$_2$, 10b. The procedure was identical to that used for **1b** using Qnz instead of Pyz. An orange powder was isolated (98.3%). IR (KBr pellet, cm^{-1}) 2122 (s), 1617 (w), 1580 (m), 1492 (m), 1379 (m), 1155 (w), 788 (m), 757 (m). Anal. Calcd for $C_{21}H_{12}N_9Cu_5$: Cu, 44.9; C, 35.62; H, 1.71; N, 17.80. Found: Cu, 44.1; C, 35.87; H, 1.72; N, 17.70. TGA Calcd for CuCN: 63.2. Found: 62.6 (180−240 °C).

(CuCN)$_2$(Pdz), 11a. The procedure was identical to that used for **1a** using Pdz instead of Pyz. Yellow-orange crystals were isolated (35.4%). IR (KBr pellet, cm^{-1}) 3086 (w), 2128 (m), 2062 (w), 1564 (w), 1443 (w), 1398 (w), 1271 (w), 1061 (w), 980 (w), 764 (m). Anal. Calcd for $C_6H_4N_4Cu_2$: Cu, 49.0; C, 27.80; H, 1.56; N, 21.61. Found: Cu, 49.0; C, 27.71; H, 1.59; N, 21.53. TGA Calcd for CuCN: 69.1. Found: 69.2 (160−210 °C).

(CuCN)$_3$(Pdz), 11b. The procedure was identical to that used for **1b** using Pdz instead of Pyz. A yellow powder was isolated (87.7%). IR (KBr pellet, cm^{-1}) 3084 (w), 2128 (m), 2064 (w), 1064 (w), 980 (w), 766 (m). Anal. Calcd for $C_7H_4N_5Cu_3$: Cu, 54.7; C, 24.11; H, 1.16; N, 20.08. Found: Cu, 54.3; C, 24.63; H, 1.20; N, 20.16. TGA Calcd for CuCN: 75.7. Found: 75.0 (140−220 °C).

(CuCN)$_5$(Ptz)$_2$, 12a. The procedure was identical to that used for **1a** using Ptz instead of Pyz. A yellow powder was isolated (48.2%). IR (KBr pellet, cm^{-1}) 2120 (s), 1450 (w), 1379 (w), 1219 (w), 924 (w), 760 (w). Anal. Calcd for $C_{21}H_{12}N_9Cu_5$: Cu, 44.9; C, 35.62; H, 1.71; N, 17.80. Found: Cu, 45.5; C, 35.97; H, 1.72; N, 17.96. TGA Calcd for $(CuCN)_4(Ptz)$: 86.2. Found: 87.7 (215−245 °C). Calcd for CuCN: 63.2. Found: 63.2 (245−275 °C).

General Method for HT Reactions. Copper(I) cyanide (4.0 or 2.0 mmol) and KCN (1.0 mmol) were suspended in 5.0 mL of H_2O in a 23-mL Teflon-lined Parr acid digestion vessel. The L ligand (1.0 mmol) was added, and the resulting suspension was stirred briefly and heated at 175 °C for 4 days. After overnight cooling to room temperature, the suspended solid was collected by means of filtration, washed with H_2O, ethanol, and diethyl ether, and then dried under vacuum. Crystals of sufficient quality for X-ray analysis were then selected.

Table 1. Synthetic Results for Aqueous Reflux and Hydrothermal Reactions

ligand	reflux 2:2:1	reflux 4:2:1	HT 2:1:1	HT 4:1:1	other
Pyz	**1a** (3:2)	**1b** (3:1)	**1a**	**1a**[b] and **1b**[b]	1:1[c]
$PyzNH_2$	**2a** (1:1)	**2b** (3:1)	–	**2d** (2:1)[a]	–
Qox	**3a** (2:1)	**3b** (3:1)	–	**3a**[b]	–
Phz	**4a** (2:1)	–	–	**4a**[b]	–
Bpy	**5a** (2:1)[b,d]	**5b** (3:1)	–	**5a** and **5d** (7:2)[b]	1:1·2Bpy,[d] 4:1[e]
Pym	**6a** (7:2)	**6a**[a]	dec	dec	–
$Pym(NH_2)$	**7a** (2:1)	**7a**	–	**7a**[a]	–
$Pym(NH_2)_2$	**8a** (2:1)	**8a**	**14**	**8d** (3:1)[a]	–
$Pym(NH_2)_3$	**9a** (3:1)	**9a**	–	**14**	–
Qnz	**10a** (2:1)	**10b** (5:2)	**13**	**10d** (4:1)[a]	–
Pdz	**11a** (2:1)[a]	**11b** (3:1)	**11a** and **11c** (2:1)[a]	**11d** (5:2)[a] and **4a**	1:1[f]
Ptz	**12a** (5:2)	**12a**	**12c** (2:1)[a]	**12d** (7:2)[a]	–

[a] New X-ray structure from sample. [b] Reference 12. [c] Reference 19. [d] Reference 13. [e] Reference 18. [f] Reference 6.

X-ray Analysis Single-crystal determinations were carried out using a Bruker *SMART Apex II* diffractometer at 100 K using graphite-monochromated Cu Kα radiation.[25] The data were corrected for Lorentz and polarization[26] effects and absorption using *SADABS*.[27] The structures were solved by use of direct methods or Patterson map. Least-squares refinement on F^2 was used for all reflections. Structure solution, refinement and the calculation of derived results were performed using the *SHELXTL*[28] package of software. The non-hydrogen atoms were refined anisotropically. For complexes **7a** and **11a**, hydrogen atoms were located by standard difference Fourier techniques and were refined with isotropic thermal parameters. In all other cases, hydrogen atoms were located and then placed in theoretical positions. In most, but not all, cases the cyano C and N atoms were disordered. When required by crystallographic symmetry, occupancies of 50% C and 50% N were used; otherwise relative C and N occupancies were refined. The former and latter cases are referred to in the text as symmetrically and non-symmetrically disordered, respectively. Complex **11c** crystallized in the chiral space group $P2_12_12_1$ but refined with a Flack parameter of 0.52(5), indicating that the sample crystal was twinned by inversion.

Powder diffraction analysis was carried out on the instrument described above. Samples were ground and prepared as mulls using Paratone N oil. Four 180-s frames were collected, covering 8−100° 2θ. Frames were merged using the *SMART Apex II* software[25] and were further processed using *DIFFRAC-Plus* and *EVA* software.[29] Simulated powder patterns from single-crystal determinations were generated using the *Mercury*[30] program.

Results

Synthesis. Copper(I) cyanide is insoluble in common solvents. Therefore, most previous strategies for preparation of CuCN:L complexes have involved either HT conditions in sealed bomb reactors or the use of acetonitrile or aqueous ammonia in order to partially solubilize the copper salt. Both acetonitrile and ammonia are well-known to coordinate Cu(I). We set out to replicate HT reactions under atmospheric aqueous reflux reactions, which are more convenient and also allow for much larger reaction scales. We used the commercial "low temperature" polymorph of CuCN,[31] which is presumably most relevant to related studies. The products listed in the first two columns of Table 1 were produced by overnight reflux of 2:2:1 or 4:2:1 mixtures of CuCN:KCN:L in water suspension. The function of the added KCN was to help solubilize the Cu(I) salts, forming hydrated species such as $K[Cu_2(CN)_3]\cdot H_2O$ (**13**),[32] which was isolated in one case from a HT reaction (see below). Despite the lack of CuCN or product solubility in water, conversions to single-phase products were consistently effected. Only in the case of the very hydrophobic L = Phz was it necessary to modify the solvent to 50% aqueous ethanol in order to accomplish coordination.

Reflux reactions produced CuCN:L networks in a variety of ratios, including 1:1, 3:2, 2:1, 5:2, 3:1 and 7:2. In the case of L = Pym, $PymNH_2$, $Pym(NH_2)_2$, $Pym(NH_2)_3$, and Ptz, 2:2:1 and 4:2:1 ratios yielded identical products as confirmed by elemental analysis and X-ray powder diffraction. More often, however, the 2:2:1 reflux reactions produced relatively low Cu products, usually $(CuCN)_2L$, and the 4:2:1 reflux reactions produced higher Cu products, usually $(CuCN)_3L$. The reflux products were typically formed as microcrystalline powders, with the exception of products **1a**, **6b**, and **11a**, which yielded X-ray-quality crystals. Most of these aromatic ligands produced colored materials, presumably owing to facile metal-to-ligand charge transfer. However, $PymNH_2$, $Pym(NH_2)_2$, and $Pym(NH_2)_3$ yielded colorless materials. In general, synthetic yields were only fair for the 2:2:1 conditions, but were better for the more copper-rich 4:2:1 conditions.

Since HT reactions are more apt to produce X-ray-quality crystals, this technique was applied in the numerous cases where no HT products yet appear in the literature. As shown in Table 1, two CuCN:KCN:L ratios (2:1:1 and 4:1:1) were again used. Less KCN was considered necessary, owing to the greater solubilizing effect of HT conditions. Product mixtures were apparent in many of the HT reactions. (This is one of the principal drawbacks of the HT technique.) Therefore, no attempt was made to quantify the results of the HT syntheses. These HT reactions led to the determi-

(25) *SMART Apex II*, Data Collection Software, version 2.1; Bruker AXS Inc.: Madison, WI, 2005.
(26) *SAINT Plus*, Data Reduction Software, version 7.34a; Bruker AXS Inc.: Madison, WI, 2005.
(27) Sheldrick, G. M. *SADABS*; University of Göttingen: Göttingen, Germany, 2005.
(28) *SHELXTL PC*, version 6.12; Bruker AXS Inc.: Madison, WI, 2005.
(29) *DIFFRAC Plus*, version 10.0 and *EVA*, release 2004; Bruker AXS Inc.: Madison, WI, 2005.
(30) *Mercury*, version 1.5: Cambridge Crystallographic Data Centre: Cambridge, UK, 2006.
(31) Hibble, S. J.; Eversfield, S. G.; Cowley, A. R.; Chippendale, A. M. *Angew. Chem., Int. Ed.* **2004**, *43*, 628.
(32) Cromer, D. T.; Larson, A. C. *Acta. Crystallogr.* **1962**, *15*, 397.

nation of eight new CuCN-based networks: **2d**, **7a**, **8d**, **10d**, **11c**, **11d**, **12c**, and **12d**. In addition, structures of **6a** and **11a** were determined from crystals isolated from reflux reactions. In order to determine the chemical and structural identity of as many aqueous reflux products as possible, X-ray powder diffraction patterns were calculated from existing or new crystal structures. These patterns were compared to powder diffractograms from the reflux products.

For CuCN products with pyrazine-like ligands, aqueous reflux replicated the known products of HT reactions for $(CuCN)_2(Qox)$ (**3a**)[12] and $(CuCN)_2(Phz)$ (**4a**).[12] Aqueous reflux reactions using 2:2:1 and 4:2:1 CuCN:KCN:Pyz stoichiometry produced $(CuCN)_3(Pyz)_2$ (**1a**) and $(CuCN)_3(Pyz)$ (**1b**), respectively. However, the powder diffraction pattern of **1b** did not match that of the previously reported HT product $(CuCN)_3(Pyz)$,[12] and therefore the reflux product may represent a new phase. However, this cannot be claimed unequivocally. The $PyzNH_2$ reflux products $(CuCN)(PyzNH_2)$ (**2a**) and $(CuCN)_3(PyzNH_2)$ (**2b**) were distinct from the structurally characterized HT product, $(CuCN)_2(PyzNH_2)$ (**2d**). Several different CuCN−Bpy networks from HT reactions, showing CuCN:Bpy ratios of 1:1·2Bpy (containing both bound and unbound Bpy), 2:1, 7:2, and 4:1, have been previously reported.[12,13,18] Aqueous reflux at 2:2:1 produced a material whose X-ray diffraction pattern matched that of $(CuCN)_2(Bpy)$, **5a**.[12,13] However, reflux at 4:2:1 produced a new stoichiometry, $(CuCN)_3(Bpy)$, **5b**.

Reflux reactions of CuCN with pyrimidine and related ligands produced the following networks: $(CuCN)_7(Pym)_2$ (**6a**), $(CuCN)_2(PymNH_2)$ (**7a**), $(CuCN)_2(Pym(NH_2)_2)$ (**8a**), $(CuCN)_3(Pym(NH_2)_3)$ (**9a**), $(CuCN)_2(Qnz)$ (**10a**), and $(CuCN)_5(Qnz)_2$ (**10b**). In addition, complexes **7a**, $(CuCN)_3(Pym(NH_2)_2)$ (**8d**), and $(CuCN)_4(Qnz)$ (**10d**) were formed as crystals through HT synthesis. The 2:1:1 HT reaction using Qnz-produced crystals of the mixed metal−cyanide network, $K[Cu_2(CN)_3]\cdot H_2O$ (**13**).[32] The 2:1:1 HT $Pym(NH_2)_2$ and the 4:1:1 HT $Pym(NH_2)_3$ reactions produced crystals of the hydrated copper(I) cyanide material, $(CuCN)_3\cdot H_2O$ (**14**).[33]

Reflux and HT reactions using Pdz and Ptz produced particularly rich product arrays. In the former case, these included $(CuCN)_2(Pdz)$ (**11a** and **11c**), $(CuCN)_3(Pdz)$ (**11b**), and $(CuCN)_5(Pdz)_2$ (**11d**), all of which except for **11b** were characterized as crystal structures. A 1:1 (CuCN)(Pdz) phase has previously been structurally characterized.[6] Crystals of two distinct $(CuCN)_2(Pdz)$ phases, **11a** and **11c**, were identified in the 2:1:1 HT mixture. On the other hand, the crystals that comprised the 2:2:1 reflux product were exclusively **11a** (as confirmed by powder diffraction). Surprisingly, red crystals of the Phz complex **4a** were found along with the yellow crystals of **11d** in the 4:1:1 HT reaction with Pdz. The conversion Pdz → Phz is unprecedented. Three Ptz complexes $(CuCN)_5(Ptz)_2$ (**12a**), $(CuCN)_2(Ptz)$ (**12c**), and $(CuCN)_7(Ptz)_2$ (**12d**) were isolated; the latter two, from HT reactions, were structurally determined.

(33) Kildea, J. D.; Skelton, B. W.; White, A. H. *Aust. J. Chem.* **1985**, *38*, 1329.

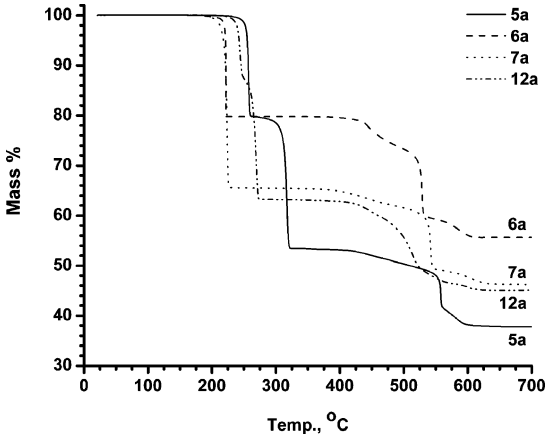

Figure 1. TGA traces for several CuCN:L networks.

Table 2. Luminescence Results

complex[a]	λ_{max} excitation[b]	λ_{max} emission	relative intensity
CuCN	285, 365*	392	14100
$(CuCN)_2(Bpy)$, **5a**	371	530	399
$(CuCN)_3(Bpy)$, **5b**	371	549	335
$(CuCN)_7(Pym)_2$, **6a**	380	520	115
$(CuCN)_2(Pdz)$, **11a**	438	571	699
$(CuCN)_5(Ptz)_2$, **12a**	370	522	747

[a] Other complexes had no luminescence response. [b] More intense band indicated by *.

Thermal Analysis. Thermogravimetric analysis (TGA) was carried out on all of the reflux products. Mass losses, temperature ranges, and interpretations are found in the Experimental Section. Several representative TGA traces are shown in Figure 1. With the exception of the $Pym(NH_2)_2$, and $Pym(NH_2)_3$ complexes (**8a** and **9a**), the TGA traces revealed smooth loss of L, sometimes occurring in multiple stages, but always leaving CuCN. This process began at temperatures as low as 125 °C and as high as 215 °C, but typically commenced around 160−180 °C. In all cases, the multistep decomposition of CuCN began at about 400 °C. Complexes of Pyz, $PyzNH_2$, Bpy, and Ptz showed plateaus prior to the ultimate formation of CuCN. Based upon TGA mass percent values, transformations 1−5 are suggested:

$$(CuCN)_3(Pyz)_2(\mathbf{1a}) \rightarrow (CuCN)_3(Pyz)(\mathbf{1b}) \rightarrow CuCN \quad (1)$$

$$(CuCN)(PyzNH_2)(\mathbf{2a}) \rightarrow (CuCN)_2(PyzNH_2)(\mathbf{2d}) \rightarrow CuCN \quad (2)$$

$$(CuCN)_2(Bpy)(\mathbf{5a}) \rightarrow (CuCN)_7(Bpy)_2 \rightarrow CuCN \quad (3)$$

$$(CuCN)_3(Bpy)(\mathbf{5b}) \rightarrow (CuCN)_9(Bpy)_2 \rightarrow CuCN \quad (4)$$

$$(CuCN)_5(Ptz)_2(\mathbf{12a}) \rightarrow (CuCN)_4(Ptz) \rightarrow CuCN \quad (5)$$

The intermediates suggested in reactions 1, 2, and 3 are known compositions.

Spectral Analysis. Infrared spectra were recorded for all of the reflux products. Most prominent in all cases is the cyanide stretch, occurring in the 2060−2150 cm^{-1} range. Despite the occurrence of as many as four crystallographically independent cyano groups, no more than two such

Table 3. Crystal and Structure Refinement Data

	2d	**6a**	**7a**	**8d**	**10d**	**11a**
CCDC deposit no.	642490	642495	642489	642491	642492	642493
color and habit	yellow needle	yellow plate	orange plate	colorless blade	yellow prism	yellow prism
size, mm	0.17 × 0.04 × 0.04	0.22 × 0.18 × 0.04	0.11 × 0.09 × 0.04	0.27 × 0.04 × 0.02	0.10 × 0.04 × 0.04	0.33 × 0.15 × 0.10
formula	$C_6H_5Cu_2N_5$	$C_{7.5}H_4Cu_{5.5}N_{3.5}$	$C_7H_{10}Cu_4N_{10}$	$C_6H_6Cu_2N_6$	$C_{12}H_6Cu_4N_6$	$C_6H_4Cu_2N_4$
formula weight	274.23	393.55	488.41	289.25	488.39	259.21
space group	$P2_1/c$ (no. 14)	$P\bar{1}$ (no. 2)	$P\bar{1}$ (no. 2)	$P2_1/c$ (no. 14)	$P\bar{1}$ (no. 2)	$C2/c$ (no. 15)
a, Å	6.9992(2)	6.78780(10)	7.4360(7)	3.68040(10)	9.0092(4)	6.92800(10)
b, Å	14.9522(5)	8.77390(10)	8.9955(8)	16.4431(6)	9.2401(7)	14.6097(2)
c, Å	8.0418(3)	9.33840(10)	12.8669(10)	16.9043(6)	10.0496(4)	8.05920(10)
α, deg	90	91.8460(10)	80.271(5)	90	106.253(4)	90
β, deg	91.873(2)	97.9390(10)	87.092(5)	90.707(2)	115.356(3)	109.2010(10)
γ, deg	90	108.8150(10)	72.335(4)	90	97.651(4)	90
volume, Å^3	841.15(5)	519.638(11)	808.30(12)	1022.92(6)	694.23(7)	770.342(18)
Z	4	2	2	4	2	4
ρ_{calc}, g cm^{-3}	2.165	2.515	2.007	1.878	2.336	2.235
F_{000}	536	378	476	568	472	504
μ(Cu Kα), mm^{-1}	5.872	7.995	5.999	4.896	6.914	6.321
radiation (*λ*, Å)	Cu Kα (1.54178)	Cu Kα (1.54178)	Cu Kα (1.54178)	Cu Kα (1.54178)	Cu Kα (1.54178)	Cu Kα (1.54178)
temperature, K	100	100	100	100	100	100
residuals:[a] *R*; R_w	0.0248; 0.0629	0.0329; 0.0838	0.0244; 0.0629	0.0378; 0.0856	0.0370; 0.0907	0.0216; 0.0559
goodness of fit	1.031	1.141	1.048	1.175	1.030	1.153

	11c	**11d**	**12c**	**12d**
CCDC deposit no.	642497	642496	642494	642498
color and habit	orange block	yellow plate	yellow prism	yellow block
size, mm	0.12 × 0.12 × 0.10	0.10 × 0.09 × 0.02	0.17 × 0.08 × 0.06	0.13 × 0.09 ×0.06
formula	$C_6H_4Cu_2N_4$	$C_{13}H_8Cu_5N_9$	$C_{10}H_6Cu_2N_4$	$C_{23}H_{12}Cu_7N_{11}$
formula weight	259.21	607.98	309.27	887.22
space group	$P2_12_12_1$ (no. 19)	$P2_1/n$ (no. 14)	$C2/c$ (no. 15)	$P2_1/n$ (no. 14)
a, Å	7.1652(14)	8.3799(2)	12.3183(2)	10.6409(2)
b, Å	7.6387(15)	14.3310(4)	10.4748(2)	10.8040(2)
c, Å	29.683(6)	14.1163(4)	9.1013(2)	12.5718(2)
α, deg	90	90	90	90
β, deg	90	96.151(2)	116.8540(10)	108.4290(10)
γ, deg	90	90	90	90
volume, Å^3	1624.6(6)	1685.50(8)	1047.71(3)	1371.19(4)
Z	8	4	4	2
ρ_{calc}, g cm^{-3}	2.120	2.396	1.961	2.149
F_{000}	1008	1176	608	860
μ(Cu Kα), mm^{-1}	5.995	7.139	4.786	6.165
radiation (*λ*, Å)	Cu Kα (1.54178)	Cu Kα (1.54178)	Cu Kα (1.54178)	Cu Kα (1.54178)
temperature, K	100	100	100	100
residuals:[a] *R*; R_w	0.0440; 0.1010	0.0441; 0.1002	0.0205; 0.0562	0.0246; 0.0627
goodness of fit	1.253	1.014	1.164	1.048

[a] $R = R_1 = \sum||F_o| - |F_c||/\sum|F_o|$ for observed data only. $R_w = wR2 = \{\sum[w(F_o^2 - F_c^2)^2]/\sum[w(F_o^2)^2]\}^{1/2}$ for all data.

bands were seen for any of the complexes. A recent analysis of IR behavior in amine base-coordinated CuCN complexes showed an inverse correlation between C≡N stretching frequency and Cu−X (X = C/N) bond length.[24] Accordingly, in the present study it was noted that in each case where weak cyano bridging produced a long copper−cyanide interaction of >2.0 Å, a band of <2100 cm^{-1} was present in the IR spectrum. This was the case for complexes **5a**,[12] **6a**, and **11a**.

Copper(I) cyanide shows moderate solid-state luminescence behavior, having a broad excitation peak in the range 250−375 nm and an fairly sharp emission peak centered at 392 nm. Semiquantitative measurements of solid-state reflectance at ambient temperature on ground powders from the reflux reactions revealed that this luminescence is largely quenched by the diimine ligands. The only instances for which greater than baseline luminescence was observed were provided by complexes **5a**, **5b**, **6a**, **11a**, **11b**, and **12a**, see Table 2. These compounds show broad excitation features in the near UV, extending into the visible range. Luminescence response for the complexes is red-shifted and is significantly reduced compared to that of CuCN under

Table 4. Selected Bond Lengths and Angles for **2d**

bond lengths (Å)		bond angles (deg)	
Cu(1)−N(2)	1.945(2)	N(2)−Cu(1)−C(1)′	112.03(11)
Cu(1)−C(1)′	2.003(3)	N(2)−Cu(1)−N(4)	112.83(9)
Cu(1)−N(4)	2.049(2)	C(1)′−Cu(1)−N(4)	111.05(10)
Cu(1)−C(1)	2.167(3)	N(2)−Cu(1)−C(1)	111.21(10)
Cu(1)−Cu(1)′	2.4411(7)	C(1)′−Cu(1)−C(1)	108.46(9)
Cu(2)−N(1)	1.956(2)	N(4)−Cu(1)−C(1)	100.64(10)
Cu(2)−C(2)′	2.006(3)	N(1)−Cu(2)−C(2)′	109.69(10)
Cu(2)−N(3)	2.042(2)	N(1)−Cu(2)−N(3)	111.98(9)
Cu(2)−C(2)	2.173(3)	C(2)′−Cu(2)−N(3)	115.13(10)
Cu(2)−Cu(2)′	2.4209(7)	N(1)−Cu(2)−C(2)	106.70(10)
N(1)−C(1)	1.157(4)	C(2)′−Cu(2)−C(2)	109.32(9)
N(2)−C(2)′	1.153(4)	N(5)−Cu(2)−C(2)	103.49(10)
		C(1)−N(1)−Cu(2)	165.9(2)
		C(2)′−3-N(2)−Cu(1)	170.1(2)
		N(1)−C(1)−Cu(1)′	153.7(2)
		N(1)−C(1)−Cu(1)	134.1(2)
		Cu(1)′−C(1)−Cu(1)	71.54(9)
		N(2)′−C(2)−Cu(2)′	155.6(2)
		N(2)′−C(2)−Cu(2)	133.3(2)
		Cu(2)′−C(2)−Cu(2)	70.68(9)

Table 5. Selected Bond Lengths and Angles for **6a**

bond lengths (Å)		bond angles (deg)	
Cu(1)−X(4)	1.872(3)	X(4)−Cu(1)−N(2)	137.56(12)
Cu(1)−N(2)	1.917(3)	X(4)−Cu(1)−N(5)	117.77(11)
Cu(1)−N(5)	2.088(3)	N(2)−Cu(1)−N(5)	103.35(10)
Cu(1)−Cu(1)′	2.9303(9)	X(3)−Cu(2)−X(1)	132.11(11)
Cu(2)−X(3)	1.916(3)	X(3)−Cu(2)−N(6)	111.20(11)
Cu(2)−X(1)	1.932(3)	X(1)−Cu(2)−N(6)	110.29(11)
Cu(2)−N(6)	2.096(3)	X(3)−Cu(2)−X(3)′	105.41(10)
Cu(2)−X(3)′	2.491(3)	X(1)−Cu(2)−X(3)′	91.55(10)
Cu(2)−Cu(2)′	2.7091(9)	N(6)−Cu(2)−X(3)′	97.75(10)
Cu(2)−Cu(3)	2.7957(6)	X(4)−Cu(3)−C(2)	155.28(12)
Cu(3)−X(4)	1.871(3)	X(4)−Cu(3)−X(1)	100.96(11)
Cu(3)−C(2)	1.877(3)	C(2)−Cu(3)−X(1)	102.58(11)
Cu(3)−X(1)	2.386(3)	X(3)−Cu(4)−X(3)′	180
Cu(3)−Cu(4)	2.7764(5)	X(1)′−X(1)−Cu(2)	174.4(3)
Cu(4)−X(3)	1.857(3)	X(1)′−X(1)−Cu(3)	105.6(3)
Cu(4)−Cu(3)′	2.7764(5)	Cu(2)−X(1)−Cu(3)	79.94(10)
X(1)−X(1)′	1.169(6)	C(2)−N(2)−Cu(1)	173.0(3)
N(2)−C(2)	1.140(4)	N(2)−C(2)−Cu(3)	179.7(3)
X(3)−X(3)′	1.159(4)	X(3)′−X(3)−Cu(4)	176.7(2)
X(3)−Cu(2)′	2.491(3)	X(3)′−X(3)−Cu(2)	169.7(3)
X(4)−X(4)′	1.154(4)	X(3)′−X(3)−Cu(2)′	115.7(2)
		Cu(2)−X(3)−Cu(2)′	74.59(10)
		X(4)′−X(4)−Cu(3)	167.1(2)
		X(4)′−X(4)−Cu(1)	176.2(3)

Table 6. Selected Bond Lengths and Angles for **7a**

bond lengths (Å)		bond angles (deg)	
Cu(1)−X(3)′	1.897(2)	X(3)′−Cu(1)−X(4)	121.24(9)
Cu(1)−X(4)	1.932(2)	X(3)′−Cu(1)−N(5)	118.70(8)
Cu(1)−N(5)	2.0284(18)	X(4)−Cu(1)−N(5)	120.05(9)
Cu(1)−Cu(3)	3.0411(6)	X(1)−Cu(2)−X(2)	122.05(9)
Cu(2)−X(1)	1.906(2)	X(1)−Cu(2)−N(8)	115.82(8)
Cu(2)−X(2)	1.910(2)	X(2)−Cu(2)−N(8)	122.08(8)
Cu(2)−N(8)	2.0241(18)	X(1)−Cu(3)−X(4)	142.71(9)
Cu(3)−X(1)	1.897(2)	X(1)−Cu(3)−N(7)	114.34(8)
Cu(3)−X(4)	1.901(2)	X(4)−Cu(3)−N(7)	102.61(8)
Cu(3)−N(7)	2.1284(18)	X(2)−Cu(4)−X(3)	142.26(9)
Cu(4)−X(2)	1.892(2)	X(2)−Cu(4)−N(10)	102.20(8)
Cu(4)−X(3)	1.895(2)	X(3)−Cu(4)−N(10)	115.42(8)
Cu(4)−N(10)	2.1184(18)		

Table 7. Selected Bond Lengths and Angles for **8d**

bond lengths (Å)		bond angles (deg)	
Cu(1)−X(1)	1.881(5)	X(1)−Cu(1)−N(3)	130.29(16)
Cu(1)−N(3)	1.937(4)	X(1)−Cu(1)−N(4)	127.10(16)
Cu(1)−N(4)	2.035(4)	N(3)−Cu(1)−N(4)	102.50(14)
Cu(2)−X(2)	1.891(4)	X(2)−Cu(2)−C(3)	126.19(17)
Cu(2)−C(3)	2.052(5)	X(2)−Cu(2)−C(3)′	122.67(17)
Cu(2)−C(3)′	2.072(5)	X(2)−Cu(3)−X(1)	122.73(16)
Cu(2)−Cu(2)′	2.3401(13)	X(2)−Cu(3)−N(5)	119.41(15)
Cu(3)−X(2)	1.926(4)	X(1)−Cu(3)−N(5)	117.17(14)
Cu(3)−X(1)	1.938(4)	X(1)−X(1)−Cu(1)	175.6(4)
Cu(3)−N(5)	2.075(4)	X(1)−X(1)−Cu(3)	177.7(4)
X(1)−X(1)	1.157(6)	X(2)′−X(2)−Cu(2)	174.4(4)
X(2)−X(2)′	1.166(6)	X(2)′−X(2)−Cu(3)	175.3(4)
N(3)−C(3)	1.142(6)	C(3)−N(3)−Cu(1)	175.2(3)
		N(3)−C(3)−Cu(2)	149.4(4)
		N(3)−C(3)−Cu(2)′	141.1(4)
		Cu(2)−C(3)−Cu(2)′	69.14(15)

identical conditions. In contrast, the luminescence emission of CuCN:diamine complexes is somewhat less shifted and often shows substantial intensity.[5]

X-ray Structures. Ten new X-ray structures emerged from the current study. Refinement details for all structures are summarized in Table 3, and selected bond lengths and angles are given in Tables 4−13. Compound **2d** crystallizes in the monoclinic space group $P2_1/c$. Both independent cyano groups are fully ordered. The X-ray structure of **2d** is

Table 8. Selected Bond Lengths and Angles for **10d**

bond lengths (Å)		bond angles (deg)	
Cu(1)−C(4)	1.897(4)	C(4)−Cu(1)−X(1)	139.63(17)
Cu(1)−X(1)	1.901(4)	C(4)−Cu(1)−N(7)	109.28(14)
Cu(1)−N(7)	2.046(3)	X(1)−Cu(1)−N(7)	110.97(15)
Cu(1)−Cu(2)	2.5412(8)	N(3)−Cu(2)−X(2)	147.19(16)
Cu(2)−N(3)	1.869(3)	C(3)−Cu(3)−X(2)	132.79(16)
Cu(2)−X(2)	1.877(4)	C(3)−Cu(3)−N(6)	115.79(14)
Cu(3)−C(3)	1.902(4)	X(2)−Cu(3)−N(6)	104.58(14)
Cu(3)−X(2)	1.931(3)	C(3)−Cu(3)−C(3)′	105.72(12)
Cu(3)−N(6)	2.127(3)	X(2)−Cu(3)−C(3)′	92.30(13)
Cu(3)−C(3)′	2.544(4)	N(6)−Cu(3)−C(3)′	96.59(12)
Cu(3)−Cu(3)′	2.7326(12)	N(4)−Cu(4)−X(5)	160.69(16)
Cu(3)−Cu(4)	2.8482(9)	X(1)′−N(1)−Cu(1)	177.4(5)
Cu(4)−N(4)	1.863(4)	X(2)′−X(2)−Cu(2)	175.0(3)
Cu(4)−X(5)	1.864(4)	X(2)′−X(2)−Cu(3)	176.6(3)
X(1)−X(1)′	1.151(7)	C(3)−N(3)−Cu(2)	167.9(3)
X(2)−X(2)′	1.155(5)	N(3)−C(3)−Cu(3)	170.9(3)
N(3)−C(3)	1.159(5)	N(3)−C(3)−Cu(3)′	112.2(3)
C(3)−Cu(3)′	2.544(4)	C(4)′−N(4)−Cu(4)	170.2(3)
N(4)−C(4)′	1.158(5)	N(4)′−C(4)−Cu(1)	169.9(4)
X(5)−X(5)′	1.146(7)	X(5)′−X(5)−Cu(4)	177.0(5)
		Cu(3)−C(3)−Cu(3)′	74.28(12)

Table 9. Selected Bond Lengths and Angles for **11a**

bond lengths (Å)		bond angles (deg)	
Cu(1)−X(2)	1.923(2)	X(2)−Cu(1)−X(1)	124.07(9)
Cu(1)−X(1)	1.934(2)	X(2)−Cu(1)−N(3)	103.45(7)
Cu(1)−N(3)	2.0788(17)	X(1)−Cu(1)−N(3)	112.86(8)
Cu(1)−X(1)′	2.300(2)	X(2)−Cu(1)−X(1)′	108.29(8)
Cu(1)−Cu(1)′	2.6597(6)	X(1)−Cu(1)−X(1)′	102.70(7)
X(1)−X(1)′	1.159(4)	N(3)−Cu(1)−X(1)′	103.78(7)
X(1)−Cu(1)′	2.300(2)	X(1)′−X(1)−Cu(1)	168.5(2)
X(2)−X(2)′	1.168(5)	X(1)′−X(1)−Cu(1)′	112.90(14)
		X(2)′−X(2)−Cu(1)	178.11(17)
		Cu(1)−N(1)−Cu(1)′	77.30(7)

Table 10. Selected Bond Lengths and Angles for **11c**

bond lengths (Å)		bond angles (deg)	
Cu(1)−X(4)	1.887(7)	X(4)−Cu(1)−X(1)	131.8(3)
Cu(1)−X(1)	1.910(6)	X(4)−Cu(1)−N(5)	124.2(2)
Cu(1)−N(5)	2.054(6)	X(1)−Cu(1)−N(5)	102.3(2)
Cu(2)−X(1)	1.873(7)	X(1)−Cu(2)−X(2)	141.0(3)
Cu(2)−X(2)	1.883(7)	X(1)−Cu(2)−N(6)	109.3(3)
Cu(2)−N(6)	2.072(6)	X(2)−Cu(2)−N(6)	109.6(2)
Cu(3)−X(2)	1.885(7)	X(2)−Cu(3)−X(3)	142.1(3)
Cu(3)−X(3)	1.889(7)	X(2)−Cu(3)−N(7)	109.8(3)
Cu(3)−N(7)	2.075(5)	X(3)−Cu(3)−N(7)	108.1(3)
Cu(4)−X(4)	1.902(7)	X(4)−Cu(4)−X(3)	131.9(3)
Cu(4)−X(3)	1.921(7)	X(4)−Cu(4)−N(8)	125.4(2)
Cu(4)−N(8)	2.049(6)	X(3)−Cu(4)−N(8)	102.3(2)
X(1)−X(1)	1.181(9)	X(1)−X(1)−Cu(1)	177.4(6)
X(2)−X(2)	1.179(9)	X(1)−X(1)−Cu(2)	176.4(6)
X(3)−X(3)	1.164(9)	X(2)−X(2)−Cu(3)	177.2(6)
X(4)−X(4)′	1.157(9)	X(2)−X(2)−Cu(2)	175.3(6)
		X(3)−X(3)−Cu(4)	176.4(6)
		X(3)−X(3)−Cu(3)	177.8(6)
		X(4)′−X(4)−Cu(1)	173.1(6)
		X(4)′−X(4)−Cu(4)	170.6(6)

depicted in Figure 2. The 3D structure is composed of 2D CuCN double sheets. The sheets are cross-linked by $PyzNH_2$ ligands which coordinate through ring nitrogen atoms. No hydrogen bonding is present. The $PyzNH_2$ groups are roughly stacked along the *c*-axis; however, alternating rings are not parallel; the angle between them is about 16.8°. The lack of coplanarity and a relatively large centroid−centroid distance (4.022 Å) suggest that π-stacking between adjacent $PyzNH_2$ should be considered minimal.[34] Copper cyanide dimer units

(34) Janiak, C. *J. Chem. Soc., Dalton Trans.* **2000**, 3885.

Table 11. Selected Bond Lengths and Angles for **11d**

bond lengths (Å)				bond angles (deg)			
Cu(1)−X(4)	1.874(6)	Cu(4)−X(1)	1.909(5)	X(4)−Cu(1)−X(3)	126.61(19)	C(5)−Cu(5)−N(9)	108.29(19)
Cu(1)−X(3)	1.971(4)	Cu(4)−N(6)	1.930(5)	X(4)−Cu(1)−N(7)	128.92(19)	X(1)′−X(1)−Cu(4)	168.0(6)
Cu(1)−N(7)	2.069(4)	Cu(4)−N(5)	1.941(5)	X(3)−Cu(1)−N(7)	99.25(17)	X(2)′−X(2)−Cu(2)	169.6(6)
Cu(2)−X(2)	1.923(5)	Cu(5)−C(6)′	1.969(6)	X(2)−Cu(2)−N(8)	103.77(19)	X(3)′−X(3)−Cu(1)	171.5(4)
Cu(2)−N(8)	2.030(4)	Cu(5)−C(5)	1.988(5)	X(2)−Cu(2)−C(5)	115.3(2)	X(3)′−X(3)−Cu(3)	178.3(5)
Cu(2)−C(5)	2.138(5)	Cu(5)−N(9)	1.992(4)	N(8)−Cu(2)−C(5)	103.36(18)	X(4)−X(4)−Cu(3)	176.7(4)
Cu(2)−C(6)′	2.340(7)	X(1)−X(1)′	1.187(10)	X(2)−Cu(2)−C(6)′	114.7(2)	X(4)−X(4)−Cu(1)	178.5(4)
Cu(2)−Cu(5)	2.3710(11)	X(2)−X(2)′	1.164(10)	N(8)−Cu(2)−C(6)′	121.7(2)	C(5)−N(5)−Cu(4)	162.5(4)
Cu(3)−X(4)	1.902(5)	X(3)−X(3)′	1.149(7)	C(5)−Cu(2)−C(6)′	98.0(2)	C(6)−N(6)−Cu(4)	177.4(5)
Cu(3)−X(3)	1.912(6)	X(4)−X(4)	1.182(7)	X(4)−Cu(3)−X(3)	141.8(2)	C(7)−N(7)−Cu(1)	117.3(3)
Cu(3)−N(10)	2.105(4)	N(5)−C(5)	1.161(7)	X(4)−Cu(3)−N(10)	110.18(18)	N(5)−C(5)−Cu(5)	150.5(4)
Cu(3)−Cu(4)	2.8594(13)	N(6)−C(6)	1.155(8)	X(3)−Cu(3)−N(10)	104.16(18)	N(5)−C(5)−Cu(2)	137.0(4)
				X(1)−Cu(4)−N(6)	121.6(2)	Cu(5)−C(5)−Cu(2)	70.05(17)
				X(1)−Cu(4)−N(5)	113.8(2)	N(6)−C(6)−Cu(5)′	157.0(6)
				N(6)−Cu(4)−N(5)	116.6(2)	N(6)−C(6)−Cu(2)′	135.9(5)
				C(6)′−Cu(5)−C(5)	117.4(3)	Cu(5)′−C(6)−Cu(2)′	66.1(2)
				C(6)′−Cu(5)−N(9)	118.0(2)		

Table 12. Selected Bond Lengths and Angles for **12c**

bond lengths (Å)		bond angles (deg)	
Cu(1)−X(1)	1.8786(19)	X(1)−Cu(1)−X(1)	132.13(8)
Cu(1)−X(1)	1.9463(16)	X(1)−Cu(1)−N(2)	127.20(7)
Cu(1)−N(2)	2.0436(15)	X(1)−Cu(1)−N(2)	100.61(7)
X(1)−X(1)′	1.154(3)	X(1)′−X(1)−Cu(1)	168.52(15)
		X(1)′−X(1)−Cu(1)	171.31(17)

Table 13. Selected Bond Lengths and Angles for **12d**

bond lengths (Å)		bond angles (deg)	
Cu(1)−X(1)	1.884(3)	X(1)−Cu(1)−X(2)	139.92(10)
Cu(1)−X(2)	1.879(3)	X(1)−Cu(1)−N(6)	110.86(9)
Cu(1)−N(6)	2.055(2)	X(2)−Cu(1)−N(6)	109.17(9)
Cu(2)−X(4)	1.906(2)	X(4)−Cu(2)−X(3)	135.65(10)
Cu(2)−X(3)	1.907(3)	X(4)−Cu(2)−N(5)	110.29(9)
Cu(2)−N(5)	2.101(2)	X(3)−Cu(2)−N(5)	106.88(9)
Cu(2)−Cu(3)	2.9696(5)	X(2)−Cu(3)−X(1)	175.52(11)
Cu(3)−X(2)	1.846(3)	X(3)−Cu(4)−X(3)′	180
Cu(3)−X(1)	1.843(2)	Cu(3)′−Cu(4)−Cu(3)	180
Cu(3)−Cu(4)	2.8775(4)	X(1)−X(1)−Cu(1)	176.5(2)
Cu(4)−X(3)	1.840(2)	X(1)−X(1)−Cu(3)	173.2(2)
X(1)−X(1)	1.159(3)	X(2)′−X(2)−Cu(1)	170.1(2)
X(2)−X(2)′	1.158(3)	X(2)′−X(2)−Cu(3)	164.3(2)
X(3)−X(3)′	1.159(3)	X(3)′−X(3)−Cu(4)	164.3(2)
X(4)−X(4)′	1.160(4)	X(3)′−X(3)−Cu(2)	167.6(2)
		X(4)′−X(4)−Cu(2)	179.3(3)

of the common type A (see Chart 2) are present, although bridging is not symmetrical (see Table 14). The dimers found in the **2d** network can be described as 6-coordinate (having four CN and two L ligands), being formed from pairs of 3-coordinate copper atoms as shown in Chart 2. Copper−copper bonding is evident within the type A $Cu_2(CN)_2$ dimer units (Cu1···Cu1′ = 2.4412(7); Cu2···Cu2′ = 2.4209(7) Å). These values are significantly less than the sum of Cu···Cu van der Waals radii, which is roughly 2.8 Å,[35] and are in fact shorter than the distance in copper metal, which is 2.56 Å.[36] (The cyano-bridged copper−copper interactions observed in the compounds reported herein are summarized in Table 14.) The dimers link to form tiled $Cu_4(CN)_4$ rings in the crystallographic *a*,*c* plane.

The Pym complex, $(CuCN)_7(Pym)_2$ **6a**, crystallizes in the triclinic $P\bar{1}$ space group. It forms a self-penetrating network (Figure 3).[37] Two perpendicular sets of CuCN chains are present, one set propagating parallel to the *c*-axis and the other parallel to a vector between the *a*- and *b*-axes. The Pym ligands lie within the *b*,*c* plane and cross-link the sets of chains. The chains are composed of 3-coordinate Cu1 and Cu2 (linked to Pym) and 2-coordinate Cu3 and Cu4 atoms. The CuCN:L stoichiometry is 3.5:1 (rather than 4:1) due to the fact that Cu4 and the center point of cyano X1, X1 (X = disordered C/N) both lie on special positions and are therefore only half independent. Very weak type-A dimerization of Cu2 with X3 is in evidence (see Table 14). Additional Cu3···Cu4 interactions cross-link the chains. In the case of this structure, all four Cu···Cu bond lengths are near van der Waals distance (2.71−2.93 Å). Only one chain cyano group (C2, N2) is ordered. However, the pseudo-bridging cyano (X3, X3) is about 90% ordered with the bridging atom tending toward carbon, as is usually the case.

The 2:1 CuCN−$PymNH_2$ complex **7a** crystallizes in $P\bar{1}$ and the 3:1 $Pym(NH_2)_2$ complex **8d** crystallizes in $P2_1/c$. As is the case with **2d**, neither of these NH_2-bearing structures (see Figures 4 and 5) exhibit either metal coordination or hydrogen-bonding of the amine substituent. Both of the networks favor sheet formation with coplanar pyrimidine rings, but there are interesting differences between

Table 14. Cyano-Bridged Copper Dimer Interactions

complex	Cu···Cu (Å)	Cu−X (Å)	Cu−X−Cu (deg)	Cu−X−X (deg)
2d	2.4411(7)	2.003(3), 2.167(3)	71.54(9)	153.7(2), 134.1(2)
2d	2.4209(7)	2.006(3), 2.173(3)	70.68(9)	155.6(2), 133.3(2)
6a[a]	2.7091(9)	1.917(3), 2.491(3)	74.59(10)	169.7(3), 115.7(2)
8d	2.3401(13)	2.052(5), 2.072(5)	69.14(15)	149.4(4), 141.1(4)
10d[a]	2.7326(12)	1.902(4), 2.544(4)	74.28(12)	170.9(3), 112.2(3)
11a[a]	2.6597(6)	1.934(2), 2.300(2)	77.30(7)	168.5(2), 112.90(14)
11d	2.3710(11)	1.969(6), 2.138(5), 1.988(5), 2.340(7)	70.05(17), 66.1(2)	150.5(4), 137.0(4), 157.0(6), 135.9(5)

[a] Bridging behavior considered borderline, see text.

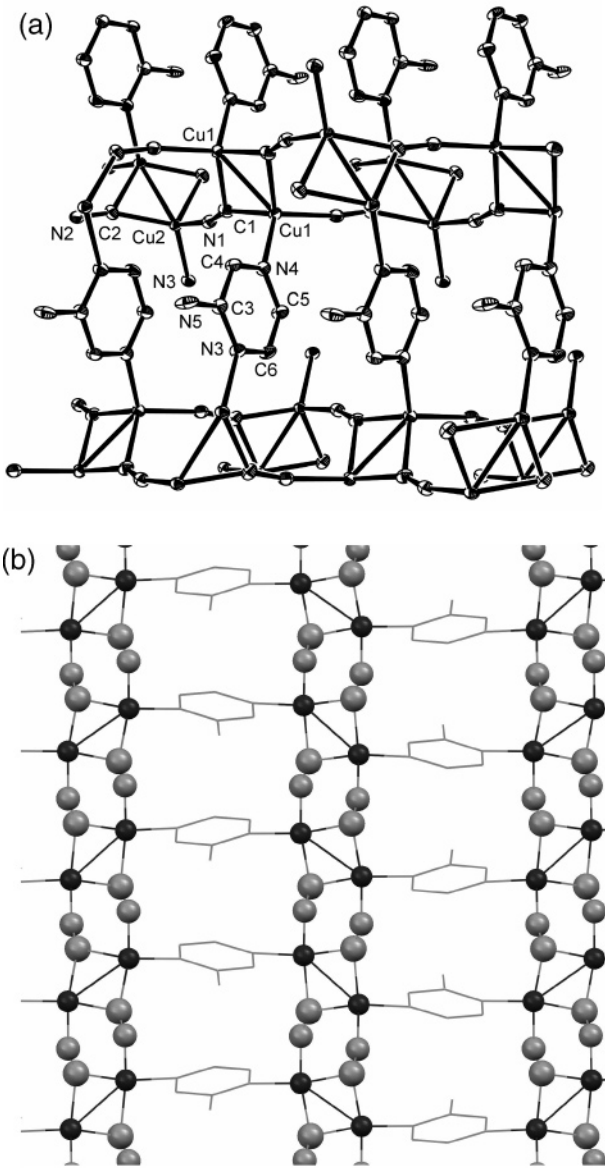

Figure 2. X-ray crystal structure of $(CuCN)_2(PyzNH_2)$, **2d**. Hydrogen atoms omitted for clarity. (a) Thermal ellipsoid view (50%). (b) Projection down crystallographic *a*-axis. Atom identities for all ball and stick projections: black circles = Cu atoms; gray circles = cyano C/N atoms; wireframe = L ligand.

them. The almost perfectly planar **7a** network is formed from tiled $Cu_6(CN)_4(PymNH_2)_2$ units (3-coordinate Cu). The network planes run parallel to the *b*-axis in the (202) crystallographic direction. All cyano groups show nonsymmetrical C/N disorder. In contrast to the fairly ordinary **7a** network, that of **8d** is very unusual. It is composed of $Cu_4(CN)_2(Pym(NH_2)_2)_2$ rings (3-coordinate Cu1 and Cu3) and type-B dimers (Cu2 and Cu4, see Chart 2). The bridging CN is the only ordered cyanide in the structure. The $(Pym(NH_2)_2)$ rings lie directly above one another and π-stack (centroid−centroid = 3.680 Å). The dimers link the aforementioned Cu_4 rings together into chains and act as pivot points for adjacent chains, which are displaced from one another by an angle of about 22.7°. These type-B dimer units are unique to our knowledge, insofar as they coordinate to only two cyano groups (i.e., they are 4-coordinate, rather than the usual 6-coordinate, dimers). It is noteworthy that the dimer Cu2···Cu2 distance is 2.3401(13) Å. This distance is remarkably short. A search of the Cambridge Crystallographic Database revealed that the proximity of the two copper centers in **8d** is surpassed by only two complexes: a highly unstable hydride-supported copper(I) dimer[38] and, interestingly, $(CuCN)_2$(tmeda) (tmeda = *N*,*N*,*N*′,*N*′-tetramethylethylenediamine).[9] The latter compound features 6-coordinate dimers in which each copper atom is chelated by a tmeda ligand and bridged by a pair of cyano groups. The Cu···Cu bond length in $(CuCN)_2$(tmeda) is a mere 2.307(2) Å.

Chart 2

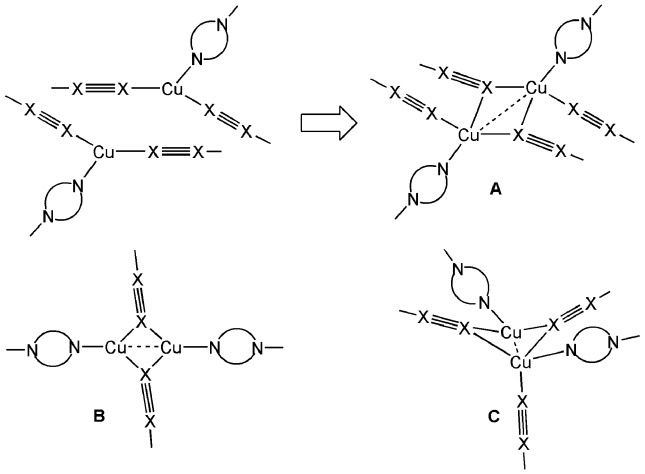

The HT reaction product $(CuCN)_4$(Qnz), **10d**, crystallizes in $P\bar{1}$. The self-penetrating 3D network structure, shown in Figure 6, comprises of two sets of CuCN chains and bears much resemblance to that of **6a** (and **12d**, see below). In one chain, propagating parallel to the *b*-axis, alternating Cu2 and Cu3 atoms are 2-coordinate and 3-coordinate, respectively, Cu3 being bonded to Qnz. In the other chain, running between the *a*- and *c*-axes, Cu4 is 2-coordinate and Cu1 is 3-coordinate. In contrast to **6a** and **12d**, all four copper atoms are fully independent, resulting in $(CuCN)_4L$ stoichiometry. The sets of CuCN chains are linked by Qnz units. π-Stacking of Qnz ligands (centroid−centroid = 3.585 Å) is evident. In addition there are two Cu···Cu interactions between CuCN chains (Cu1···Cu2 = 2.5412(8), Cu(3)···Cu(4) = 2.8482(9) Å) and, as is the case with **6a**, there is a suggestion of an asymmetrically bridged type-A dimer at Cu3 (see Table 14). One cyano group is nonsymmetrically disordered, and one pair of half cyano groups is symmetrically disordered in this structure. The two remaining cyano groups refined to distinct C and N positions.

During the course of this work, the structures of two new $(CuCN)_2$(Pdz) complexes were solved, **11a** (Figure 7) and

(35) Pyykkö, P. *Chem. Rev.* **1997**, *97*, 597.
(36) Greenwood, N. N.; Earnshaw, A. *Chemistry of the Elements*, 2nd ed.; Butterworth-Heinemann: Oxford, 1997; Chapter 28.2.3, p 1176.
(37) Batten, S. R.; Robson, R. *Angew. Chem., Int. Ed.* **1998**, *37*, 1460.
(38) Mankad, M. P.; Laitar, D. S.; Sadighi, J. P. *Organometallics* **2004**, *23*, 3369.

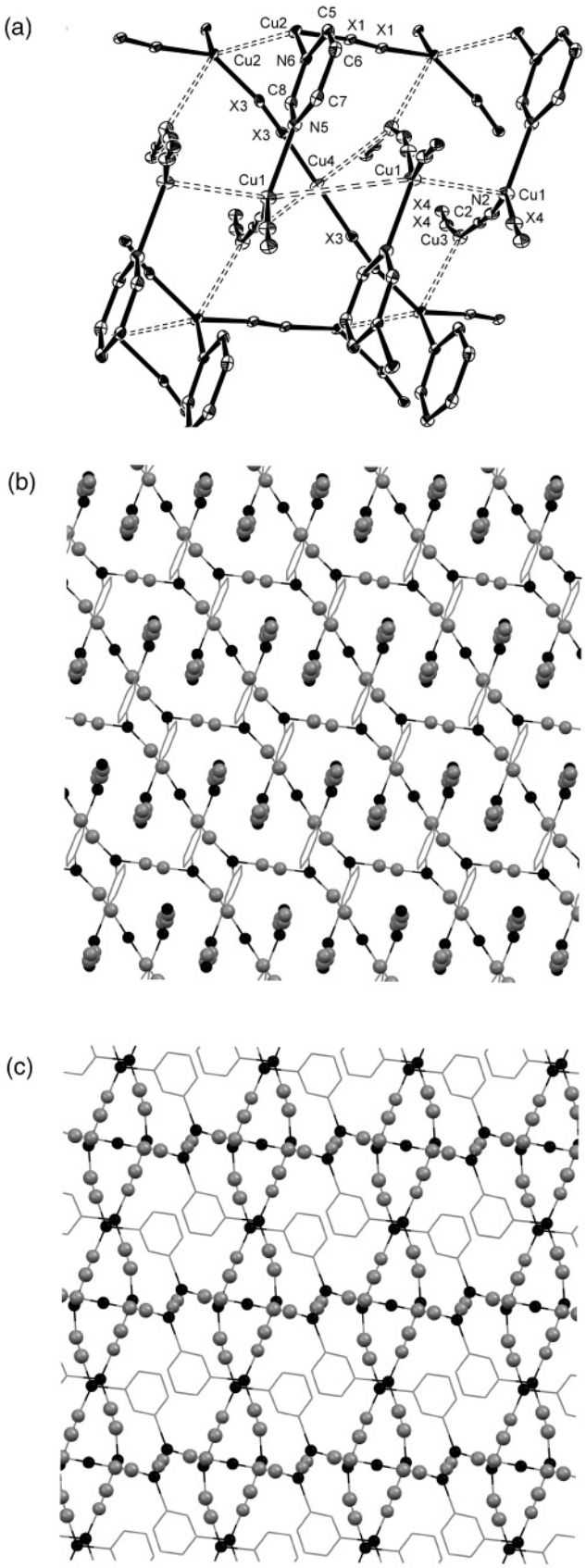

Figure 3. X-ray crystal structure of $(CuCN)_7(Pym)_2$, **6a**. Hydrogen atoms omitted for clarity (a) Thermal ellipsoid view (50%). All Cu···Cu interactions are shown with dashed bonds. (b) Projection down crystallographic *c*-axis. Cu···Cu interactions are not shown. (c) Projection down crystallographic *a*-axis. Cu···Cu interactions are not shown.

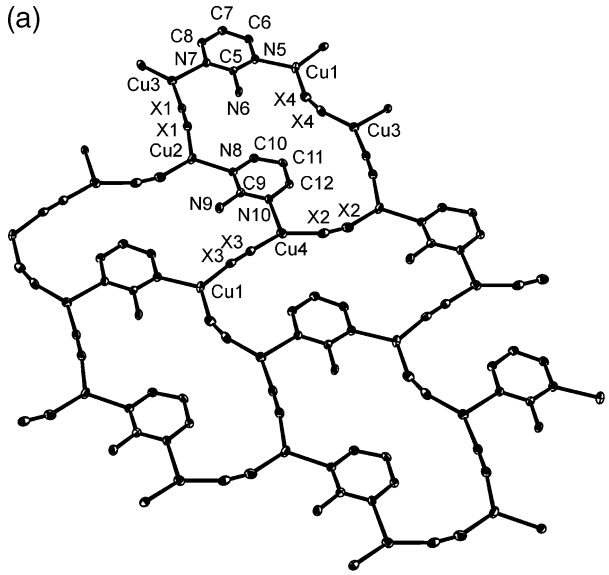

Figure 4. X-ray crystal structure of $(CuCN)_2(PymNH_2)$, **7a**. Hydrogen atoms omitted for clarity. (a) Thermal ellipsoid view (50%) projected down crystallographic *a*-axis.

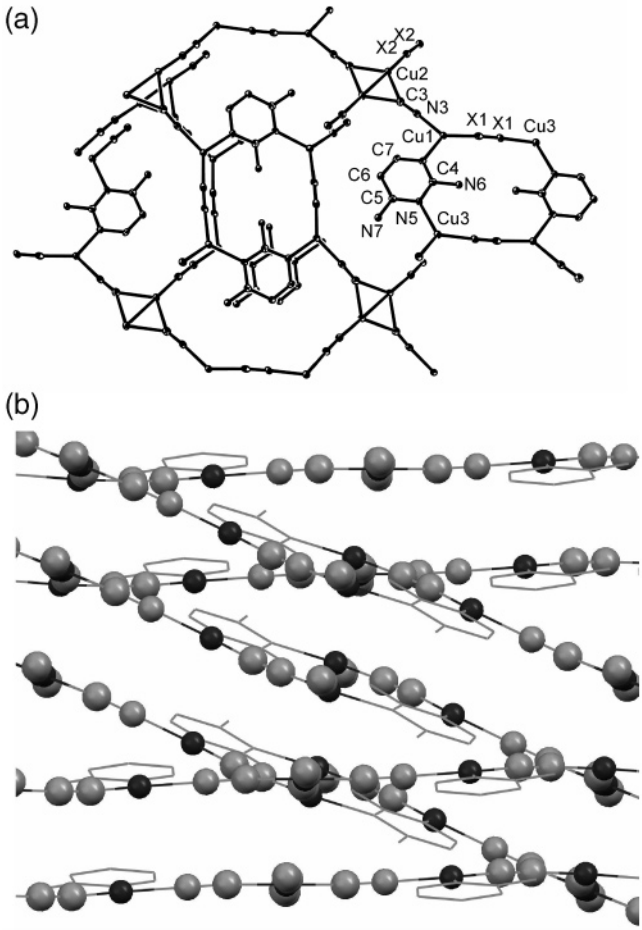

Figure 5. X-ray crystal structure of $(CuCN)_3(Pym(NH_2)_2)$, **8d**. Hydrogen atoms omitted for clarity. (a) Thermal ellipsoid view (50%). (b) Projection between crystallographic *b*- and *c*-axes showing offset sheets.

11c (Figure 8). The **11a** product crystallized in the monoclinic *C*2/*c* space group and consists of a 2D sheet network of tiled $Cu_6(CN)_4(Pdz)_2$ units parallel to the *a*,*c* plane. Pairs

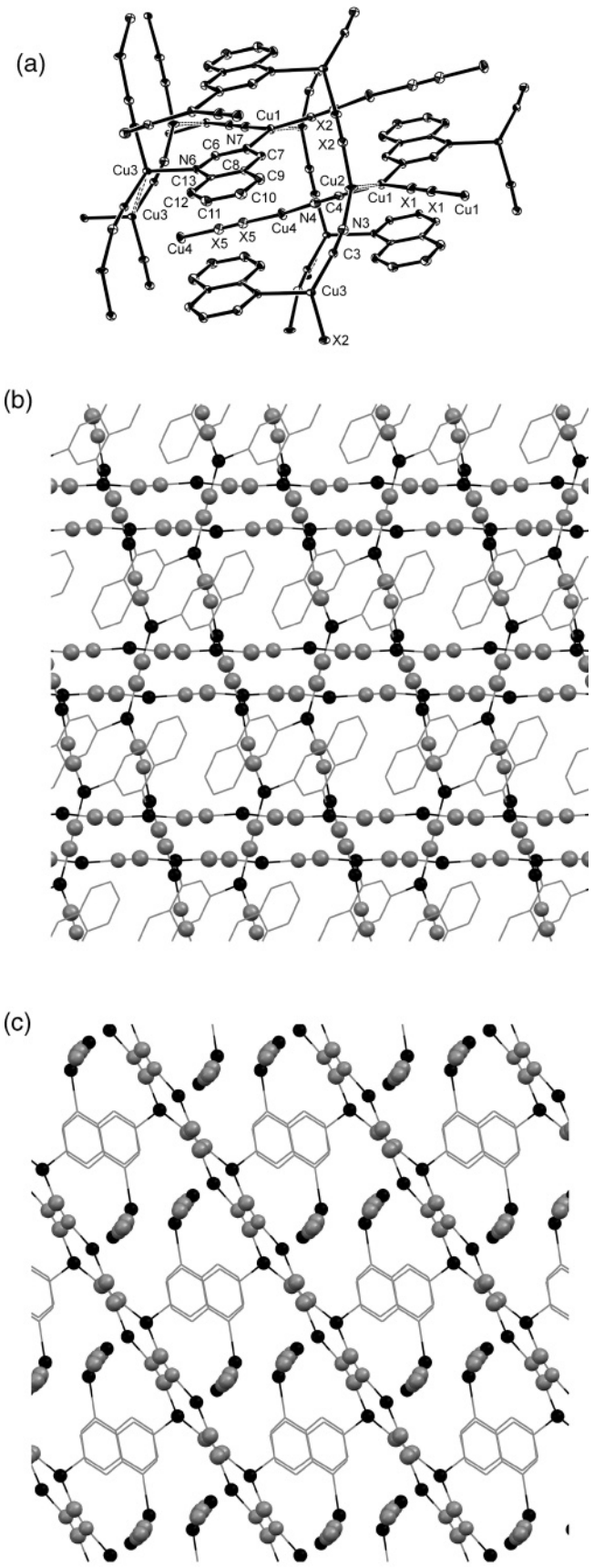

Figure 6. X-ray crystal structure of $(CuCN)_4(Qnz)$, **10d**. Hydrogen atoms omitted for clarity. (a) Thermal ellipsoid view (50%). All Cu···Cu interactions are shown with dashed bonds. (b) Projection down crystallographic *a*-axis. Cu···Cu interactions are not shown. (c) Projection down crystallographic *b*-axis, illustrating π-stacking. Cu···Cu interactions are not shown.

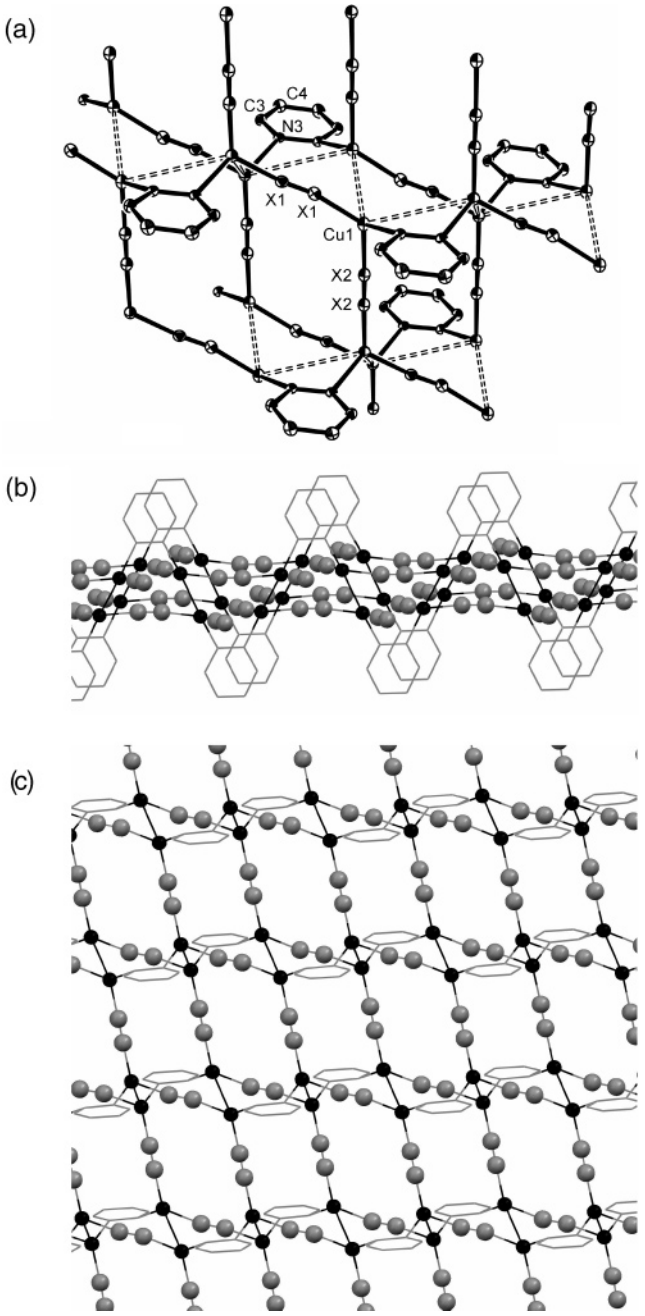

Figure 7. X-ray crystal structure of $(CuCN)_2(Pdz)$, **11a**. Hydrogen atoms omitted for clarity. (a) Thermal ellipsoid view (50%). All Cu···Cu interactions shown with dashed bonds. (b) Projection down crystallographic *a*-axis. (c) Projection down crystallographic *b*-axis.

of sheets are weakly linked together via asymmetrically bridged type-A dimers at Cu1 (see Table 14). Furthermore, pairs of dimers that are held together by a Pdz ligand also share an asymmetrically μ_4-bridging cyano unit. The Pdz ligands are interleafed between the 2D sheets, but alternating rows of Pdz groups are offset from one another, so that there is no π-stacking effect. Both independent cyano groups are symmetrically disordered. The **11c** network crystallized in the orthorhombic $P2_12_12_1$ space group as a racemic twin. It too forms 2D sheets tiled from $Cu_6(CN)_4(Pdz)_2$ rings, in this case running parallel to the *a*,*b* crystallographic plane. In contrast to **11a**, the sheets are highly rippled and are not

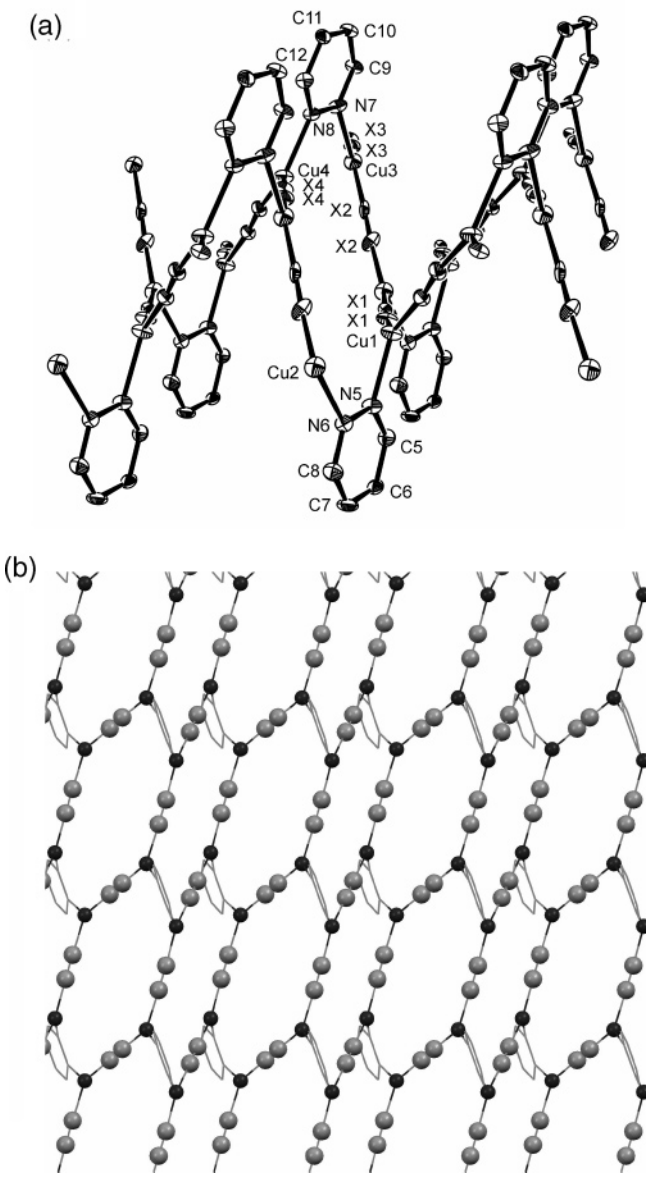

Figure 8. X-ray crystal structure of $(CuCN)_2(Pdz)$, **11c**. Hydrogen atoms omitted for clarity. (a) Thermal ellipsoid view (50%). (b) Projection down crystallographic *c*-axis.

paired, owing to the absence of dimers or Cu···Cu interactions. A relatively short, but nonbonding, Cu1···Cu2 distance within the sheet (3.187 Å) is the result of attachment to a common Pdz ligand. There is no π-stacking. All four independent CN units are nonsymmetrically disordered. The literature (CuCN)(Pdz) structure bears a close relation to both **11a** and **11c**, since it also consists of 2D tiled sheets of $Cu_6(CN)_4(Pdz)_2$ rings.[6] However, in this 1:1 structure the copper atoms are 4-coordinate, and the Pdz rings protrude above and below the sheet in perpendicular orientations. In contrast to the 2:1 networks, (CuCN)(Pdz) contains discrete $Cu_2(Pdz)_2$ units (Cu1···Cu2 = ca. 3.679 Å). In addition, the fact that each pair of copper atoms shares a pair of Pdz bridges produces a flat sheet in (CuCN)(Pdz).

A HT 5:2 Pdz complex, **11d**, crystallizes in the monoclinic space group $P2_1/n$. The structure of **11d** comprises a complicated 3D network (see Figure 9) containing both 3-

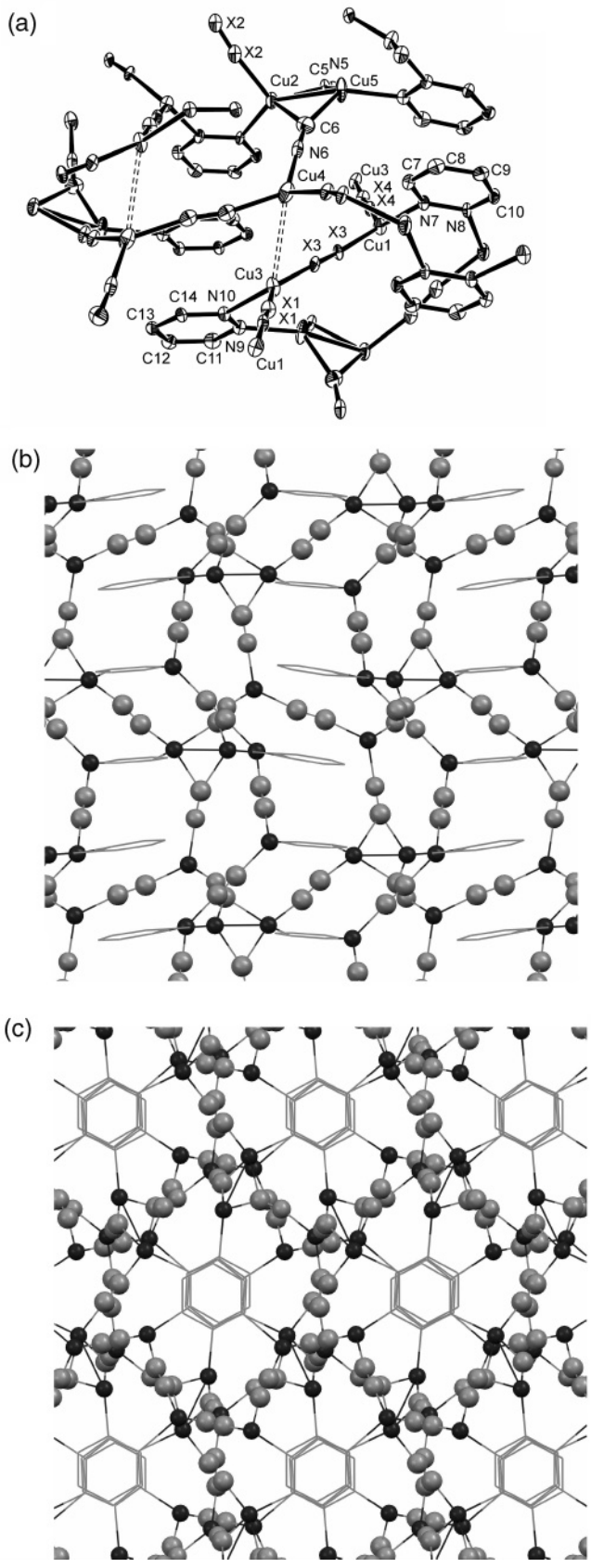

Figure 9. X-ray crystal structure of $(CuCN)_5(Pdz)_2$, **11d**. Hydrogen atoms omitted for clarity. (a) Thermal ellipsoid view (50%). Non-dimer Cu···Cu interactions are shown with dashed bonds. (b) Projection down crystallographic *a*-axis. (c) Projection down crystallographic *c*-axis, illustrating π-stacking. Non-dimer Cu···Cu interactions are not shown.

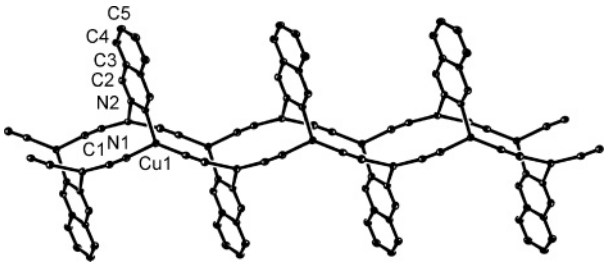

Figure 10. X-ray crystal structure of $(CuCN)_2(Ptz)$, **12c**. Hydrogen atoms omitted for clarity. Thermal ellipsoid view (50%).

and 2-coordinate metal centers. The bridging C5, N5 and C6, N6 represent the only ordered cyanides. Copper cyanide sheets running between the *b*- and *c*-axes are formed from alternating 3-coordinate (Cu4) monomeric and 5-coordinate (Cu2, Cu5) dimeric copper centers. A non-dimer Cu3···Cu4 interaction (2.8594(13) Å) is also present. The sheets are cross-linked by Pdz ligands, which coordinate to the dimers and π-stack along the *c*-axis (centroid−centroid = 3.468, 3.576 Å). The π-stacking of Pdz units involves four distinct ring rotational positions. The $Cu_2(CN)_2$ dimers found in this material are unique. In contrast to all other dimers identified in this study, this one is not composed of crystallographically equivalent copper atoms. This is the case because, in addition to the two bridging cyanides shared by the two metal centers, Cu2 coordinates to a cyano and a Pdz ligand, while Cu5 connects only to Pdz. This unique arrangement is illustrated as type-C in Chart 2. The Cu5 center shows slightly pyramidal geometry (sum of bond angles = 343.7° and elevation of Cu5 above the C5, C6, N9 plane = ca. 0.47 Å). This slight pyramidal distortion results from a long-range interaction of Cu5 with a cyanide atom (Cu5···X3 = 2.613 Å). Like the 4-coordinate type-B dimer in **8d**, the 5-coordinate type C dimer also exhibits a very short metal−metal distance (Cu2···Cu5 = 2.3710(11) Å). The dimer is bent, having an angle of 25.76° between the planes defined by Cu2, C6, Cu5 and Cu2, C5, Cu5. A search of the Cambridge Crystallographic Database revealed the Cu(5)−C(6)−Cu(2) angle of 66.1(2)° to be the fourth most acute such angle known and the most acute for a copper cyanide complex (the more acute angles belonging to alkynyl-bridged copper clusters).[39]

Although no structural information was available for 5:2 Ptz complex, **12a**, that resulted from both reflux reactions, HT synthesis generated two additional networks, $(CuCN)_2(Ptz)$ (**12c**) and the $(CuCN)_7(Ptz)_2$ (**12d**). The former network (Figure 10), which crystallizes in *C*2/*c*, consists of a simple double ladder of CuCN chains linked by Ptz "rungs" extending out from alternating sides of ladder. The ladder propagates parallel to the crystallographic *c*-axis. In similar fashion to that of complex **11a**, the ligands are interleafed between the chains, but without π-stacking. Copper atoms are 3-coordinate and are separated across the ladder by about 3.177 Å. The single cyano group present is fully ordered.

(39) (a) Higgs, T. C.; Parsons, S.; Bailey, P. J.; Jones, A. C.; McLachlan, F.; Parkin, A.; Dawson, A.; Tasker, P. A. *Organometallics* **2002**, *21*, 5692. (b) Chui, S. S. Y.; Ng, M. F. Y.; Che, C.-M. *Chem.-Eur. J.* **2005**, *11*, 1739.

Complex **12d** crystallizes in $P2_1/n$. It forms the self-penetrated 3D network shown in Figure 11. The structure bears analogy to that of **6a**, consisting of two sets of CuCN chains cross-linked by Ptz ligands. The chains run in perpendicular directions between the *a*- and *c*-axes. The Ptz rings are coplanar with series of Cu1, Cu3 chains. As is the case with **6a**, there is weak copper−copper bonding between proximal 2-coordinate copper atoms in perpendicular chains (Cu3···Cu4 = 2.8775(4) Å) and one copper atom (Cu4) and one cyano group (X4, X4) are half-independent. But unlike **6a**, there is no sign of even weak type-A dimer formation. Cyano groups in **12d** are disordered, and Ptz π-stacking is not evident.

Discussion

We set out to prove that copper(I) cyanide networks with bridging ligands could be easily synthesized under convenient aqueous reflux conditions in order to provide significant amounts of single-phase materials in good yield. The results in Table 1 (along with the yield data in the Experimental Section) confirm that we have done this. A second, more challenging, goal of the work involved better understanding the influences upon product formation of HT versus open reflux conditions. Here patterns are more difficult to discern. One of the major difficulties we encountered involved the tendency of HT conditions to produce mixtures of products, decomposition materials (e.g., copper powder), and ligand-free materials (such as **13** and **14**). Of course, these problems serve to confirm that reflux synthesis, when feasible, is the superior approach. It is apparent from the results in Table 1 that HT and reflux reactions often produce different products from one another. However, there is no clear trend toward HT formation of products that are more copper-rich, or more closely follow the nominal stoichiometry, or have higher metal coordination numbers, or any other predictable trend.

Two generalizations can safely be made with regard to the network chemistry of CuCN diimine complexes, generalizations which also apply to complexes of CuCN with diamines.[5,9] First, it is apparent that multiple stoichiometries can be, and are, obtained for any given L. We make no claim of comprehensiveness in identifying all possible CuCN networks for the L groups studied. This would necessitate investigating more mixing ratios and probably other reaction conditions. Nevertheless, despite the existence of several previous studies, numerous new networks have been identified in the present contribution, resulting in 10 new structural analyses.

The second generalization that can be readily offered is that stoichiometric and structural diversity is the rule for the CuCN network products. It is instructive to evaluate structural trends within groups of networks as defined by stoichiometry. The least copper-rich materials described herein and in the literature tend to form the simplest networks. The 1:1 complexes of CuCN with Pyz,[19] 2-MePyz,[14] and 4-MePym[14] form dense, interpenetrated 3D networks having 4-coordinate Cu centers bridged equally by CN and L. However, when L = Bpy, the larger bridge produces a network which is so porous that it has been found

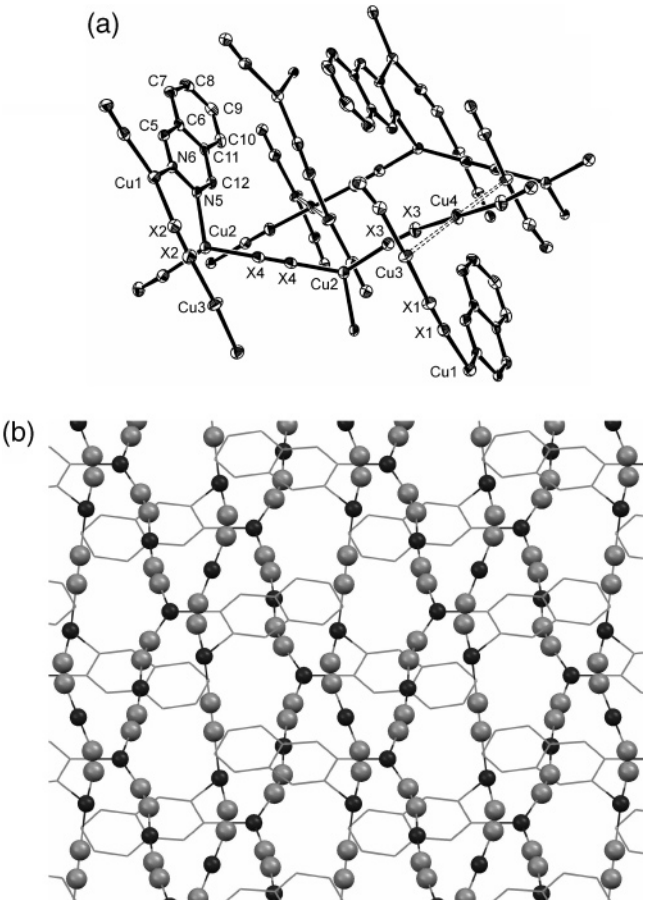

Figure 11. X-ray crystal structure of $(CuCN)_7(Ptz)_2$, **12d**. Hydrogen atoms omitted for clarity. (a) Thermal ellipsoid view (50%). All Cu···Cu interactions are shown with dashed bonds. (b) Projection down crystallographic *a*-axis. Cu···Cu interactions are not shown.

to incorporate two equivalents of free Bpy within the pores.[13] In another (CuCN)L complex (L = 1,4-bis(4-pyridyl)-*trans*-1,4-divinylbenzene), the CuCN chains and CuL chains propagate in separate directions, resulting in a highly rippled 2D sheet structure.[22] As with the other 1:1 materials, (CuCN)(Pdz) contains 4-coordinate Cu centers.[6] However, due to the geometry of the 1,2-diazine Pdz, pairs of copper atoms in adjacent CuCN chains are linked by pairs of Pdz ligands forming a 2D sheet. In the course of the current study, only **2a** was identified as a 1:1 compound. Given the small size of the $PyzNH_2$ ligand and its obvious relation to the ligands noted above, it is reasonable, in the absence of X-ray structural information, to speculate that its structural type is analogous to that of the 3D Pym and Pyz materials.

Although no new $(CuCN)_3L_2$ networks are reported in this contribution, there are three relevant structures that bear mentioning: L = Pyz (**1a**),[12] 2,3-Me_2Pyz,[15] and hexamethylenetetramine (HMTA).[7] Interestingly, there is little analogy between the three structures. The Pyz complex **1a** forms a 3D honeycomb structure of six-copper (Cu_6) rings. Half of the copper centers are 4-coordinate, and the remaining copper atoms are 2-coordinate. The 2,3-Me_2Pyz also forms a 3D net; however in this case half of the metal centers are 4-coordinate, and the rest form the familiar type-A dimers. The network is constructed of Cu_4 and Cu_6 rings. Finally, $(CuCN)_3(HMTA)_2$, in which the HMTA ligands are bidentate, is a 2D sheet structure tiled from Cu_4 and Cu_6 rings having equal numbers of 4- and 3-coordinate copper centers.

The 2:1 structures represented herein include **2d**, **3a**,[12] **4a**,[12] **5a**,[12,13] **7a**, **11a**, **11c**, and **12c**. It is useful to divide the large class of known 2:1 networks into two subclasses: those containing type-A $Cu_2(CN)_2$ dimers (with associated Cu···Cu interactions) and those without. Of course, the distinction between the two categories of $(CuCN)_2L$ networks is somewhat arbitrary since there is potentially a continuum between isolated and bridged pairs of 3-coordinate Cu(I) centers, as illustrated in Chart 2. The best criterion for making this distinction appears to be the Cu−X−X bond angle. We suggest that true dimers are present when the angle is greater than ca. 168°. We define as borderline those cases in which the Cu−X−X bond angles are >168°, but (slightly longer) Cu···Cu interactions are still present.

The bridged $(CuCN)_2L$ networks produce 3D networks since the type-A $Cu_2(CN)_2$ unit usually forms six network connections in nearly mutually perpendicular directions. Definitively bridged networks include **5a** (Cu···Cu = 2.491 Å, Cu−X−X = 163.98°)[12,13] and $(CuCN)_2L$, L = *trans*-4,4′-bipyridylethylene (Cu···Cu = 2.489 Å, Cu−X−X = 161.53°),[12] and piperazine (Cu···Cu = 2.581 Å, Cu−X−X = 151.22°).[9] A number of borderline $(CuCN)_2L$ structures are known as well: L = 2-MePyz (Cu···Cu = 2.588 Å, Cu−X−X = 170.76°),[14] L = 2-EtPyz (Cu···Cu = 2.577 Å, Cu−X−X = 171.42°),[12] L = 2,3-Me_2Pyz (Cu···Cu = 2.747 Å, Cu−X−X = 174.56°),[12] L = 2,5-Me_2Pyz (Cu···Cu = 2.645 Å, Cu−X−X = 173.80°),[12] and L = 2,6-Me_2Pyz (Cu···Cu = 2.568 Å, Cu−X−X = 171.99°).[12] These networks are invariably 3D honeycombs as a result of cross-linking of the (6,3) sheets (i.e., 6-membered rings with 3-coordinate metal centers).[37] The honeycombs consist of Cu_6 or both Cu_6 and Cu_4 ring systems. Although C/N disorder may still occur in the dimers, there appears to be a distinct preference for carbon occupancy at the metal-bridging cyanide atom position. The only new $Cu_2(CN)_2$-bridged 2:1 product is **2d**, which is a fairly typical example of a 3D honeycomb network consisting of Cu_6 and Cu_4 ring systems.

Nonbridged 2:1 compounds are almost invariably formed as 2D sheets comprised of CuCN chains linked by L. The networks formed are of the (6,3) type. In fact, 6-copper rings are extremely common in all bridged Cu(I) networks. Interestingly, a non-polymeric $(CuCN)_6L_6$ ring is known for L = the bulky PCy_3.[40] Previously characterized examples of $(CuCN)_2L$ definitively lacking dimers include **3a**,[12] **4a**,[12] and $(CuCN)_2L$, L = Me_4Pyz[12] and *N*,*N*′-dimethylpiperazine.[9] Four new complexes described herein fall in this category. Most straightforward of these is **7a** which forms a fully planar 2D structure with the $PymNH_2$ rings lying within the plane. Similar coplanarity has been noted for **3a**[12] and

(40) Lin, Y.-Y.; Lai, S.-W.; Che, C.-M.; Fu, W.-F.; Zhou, Z.-Y.; Zhu, N. *Inorg. Chem.* **2005**, *44*, 1511.

$(CuCN)_2$(2-MePyz).[14] The other new structures in this category, **11a**, **11c**, and **12c**, are formed from the 1,2-diimines Pdz and Ptz. The geometry of these ligands lends itself to formation of ladder structures. In **12c** alignment of rungs produces a simple ladder, while in **11a** and **11c** the rungs are staggered, linking multiple chains into sheets. Borderline bridging is noted in **11a**.

Complexes **10b**, **11d**, and **12a** all show 5:2 CuCN:L stoichiometry and are, to our knowledge, the such first networks. The only one of these to be structurally elucidated was **11d**, which features Pdz, a ligand that tends to impose laddering, as discussed above. Nevertheless, in this case laddering is not seen. That is, the copper centers that share a Pdz ligand are not formed into parallel chains or sheets. What is noteworthy in **11d** is the formation of novel type-C $Cu_2(CN)_2$ dimers. These 5-coordinate dimers allow for the more copper-rich half-unit ratio stoichiometry observed.

Although few 3:1 CuCN:L networks have been reported to date, seven such materials are reported in the present study: **1b**,[12] **2b**, **3b**, **5b**, **9a**, **11b**, and **8d**. Unfortunately, the only new 3:1 structure determined was that of **8d**. The more copper-rich phases favor lower coordination numbers. Sometimes this trend is represented by the occurrence of nearly independent CuCN chains. For example, the 3:1 complex **1b** is constituted from simple $(CuCN)_2L$ 2D (6,3) sheets plus CuCN chains that pass through the hexagonal channels in the sheets.[12] On the other hand the new 3:1 network, **8d** is constructed without CuCN chains. As described in the preceding section, **8d** forms a pair of 2D sheets that intersect at unusual type-B 4-coordinate $Cu_2(CN)_2$ dimer units that exhibit a remarkable degree of cuprophilic interaction.[35] To our knowledge there is no precedent for this sort of sheet or dimer structure in known Cu(I) cyano complexes.

Phases having CuCN:L ratios of 7:2 or greater can be considered highly copper-rich. Three new complexes are herein described, adding to the three that are reported in the literature. The latter include the 7:2 and 4:1 complexes of CuCN with Bpy.[13,18] Like Pyz complex **1b**, these are both based upon the (6,3) net described for $(CuCN)_2$(Bpy) (**5a**); $(CuCN)_7(Bpy)_2$ (**5d**) is interpenetrated by a single CuCN chain, and $(CuCN)_4$(Bpy) is interpenetrated by two such chains. Our TGA results for complex **5a** showed evidence for the direct conversion to **5d**, presumably via the stripping of the Bpy cross-links from sheets to leave CuCN chains. The newly identified 3:1 material, **5b**, undergoes thermal decomposition with evidence of a $(CuCN)_9(Bpy)_2$ intermediate phase. Just as the 7:2 and 4:1 CuCN:Bpy materials have been shown to contain the (6,3) net plus one and two CuCN chains, respectively, this apparent 9:2 phase could incorporate three CuCN chains with the (6,3) net.

The three new copper-rich complexes, the 7:2 **6a** and **12d** and the 4:1 **10d**, are closely related to one another. All three exhibit two sets of perpendicular CuCN chains consisting of both 2- and 3-coordinate copper centers with cross-linking by "bent" ligands. Unlike the Bpy complexes, independent CuCN chains are not observed. The distinction between the 7:2 and 4:1 ratio is a subtle one, resting upon crystallographic occupancies. In the 7:2 networks the 2-coordinate copper atom and a cyano group within one of the CuCN chains lie at special positions and thus have half occupancies. Hence, the sequence of 2- and 3-coordinate copper centers in **6a** and **12d** is ...3, 3, 2, 3, 3, 2... and that in **10d** is ...3, 3, 2, 2, 3, 3... Both **6a** and **10d** show borderline type-A bridging.

Some final comments on the prevalence of π-stacking are in order.[34] While it would seem reasonable that the diimine ligands studied would lend themselves to arene π-stacking effects, the phenomenon is clearly evident for a relatively modest subset of the present networks: **3a**,[12] **8d**, **10d**, **11d** and the related complexes (CuCN)(4-MePym),[14] $(CuCN)_2$(2-MePyz),[14] $(CuCN)_2$(2,3-Me_2Pyz),[12] and $(CuCN)_2$(2,5-Me_2Pyz).[12] More often the rings are significantly offset in adjacent layers, minimizing their approach. This effect is not surprising in 3D networks, for which formation of the bonded network will naturally outweigh any π-stacking considerations. However, even in 2D networks, such as **7a**, arene π-stacking is noteworthy by its absence. In this case adjacent layers are sufficiently displaced that any π-interactions present would be better described as being between $PymNH_2$ and cyanide. In **7a**, the centroid−X1 distances are 3.266 and 3.499 Å. Somewhat longer ring−CN interactions are noted in **11c** between the N5, N6, C5−C8 centroid and X1 (3.675 and 3.877 Å) and between the N7, N8, C9−C12 centroid and X3 (3.881 and 4.214 Å). Finally, these interactions are also seen in **12d** between the C6−C11 centroid and X2 (3.530 and 4.040 Å). The foregoing values, especially those in **7a**, are sufficiently short as to suggest a $\pi-\pi$ interaction.

Conclusion

We have explored the formation of CuCN networks with diimine ligands by both open aqueous reflux and HT methods. Although the two techniques sometimes yield identical phases, more often the products of the two methods are distinct. The products are weakly or nonluminescent, presumably as a result of the quenching of the CuCN activity by the aromatic spacer ligands. The products smoothly decompose under flowing nitrogen, ultimately yielding CuCN, but sometimes revealing copper-rich intermediate phases. The structures of CuCN-L materials vary widely. Recurrent themes include: (1) the formation of 3D networks by 4-coordinate copper, (2) formation of 2D nets (especially (6,3) nets) by 3-coordinate copper, (3) the reformation of these 3-coordinate metal centers into 6-coordinate type-A dimeric units, producing 3D networks, and (4) the formation of 2-coordinate CuCN chains or mixed 2-/3-coordinate chains at higher CuCN content. Several novel structural features have been identified, including the first $(CuCN)_5L_2$ networks, a 4-coordinate type-B dimer that features a very short Cu···Cu interaction, and a folded 5-coordinate type-C dimer having a very acute Cu−C−Cu bond angle.

Acknowledgment. Grateful acknowledgment is made to the donors of the American Chemical Society Petroleum Research Fund (44891-B3) and the Thomas F. and Kate Miller Jeffress Memorial Trust (J-678). We also acknowledge a Howard Hughes Medical Institute Grant through the Undergraduate Biological Sciences Education Program to the

College of William and Mary. We are indebted to NSF (CHE-0443345) and the College of William and Mary for the purchase of the X-ray equipment.

Supporting Information Available: Full details of the crystal structure determinations for **2d**, **6a**, **7a**, **8d**, **10d**, **11a**, **11c**, **11d**, **12c**, and **12d** in CIF format and tables of crystal data, atomic coordinates, bond lengths and angles, and anisotropic displacement parameters. This material is available free of charge via the Internet at http://pubs.acs.org.

IC7007057